

UNIVERSITÀ DEGLI STUDI DI PADOVA

Dipartimento di Fisica e Astronomia “Galileo Galilei”

Master Degree in Physics

Final Dissertation

Dark pions through the Z portal: dark Z' mediation

Thesis supervisor

Dr. Ennio Salvioni

Candidate

Marco Ferla

Academic Year 2022/2023

Contents

A map to this thesis	1
1 Introduction	3
1.1 Symmetry-based solutions of the hierarchy problem	5
1.2 Changing perspective: Neutral Naturalness, and the Twin Higgs	6
1.3 The motivation for confinement in the dark sector	10
1.4 Summary: particle content of the Fraternal Twin Higgs	11
2 Some theoretical tools	13
2.1 Chiral perturbation theory (ChPT)	13
2.1.1 Couplings to photons and axion-like particles	15
2.2 Electroweak precision tests (EWPT) of the SM	16
3 Confining dark sectors from Neutral Naturalness	19
3.1 Dark hadron phenomenology in the Fraternal Twin Higgs	19
3.2 Toward a theory of dark pions	21
3.2.1 Constraints from Z and h invisible decays	25
3.3 Hadronic decays of dark pions: an example ChPT calculation	25
4 Z' model and constraints	29
4.1 Constraints from EWPT	30
4.2 Constraints from Z invisible decays	33
5 Dark pions in the Z' model	37
5.1 The $Z - Z'$ portal for CP -odd dark pions	37
5.1.1 Comparing the two UV completions	38
5.1.2 A concrete example model	39
5.2 The $h - \phi$ portal for CP -even dark pions	40
6 Conclusions	43
Bibliography	45

A map to this thesis

The naturalness problem of the Higgs mass has been a major driver of particle physics for the past decades. However, the absence of signals from the TeV scale at the LHC Runs 1 and 2 has prompted the field to reconsider its viewpoint. This thesis is inspired by the framework of Neutral Naturalness (NN), where the hierarchy problem is still solved by symmetry – as in “traditional” approaches – but the new particles appearing at the TeV scale are rendered neutral under SM QCD, through clever implementation of discrete symmetries. A phenomenologically important and generic prediction of NN scenarios is the existence of a QCD-like dark sector that confines around the GeV scale. In this thesis, we study a dark sector model that features dark pions at the bottom of the hadron spectrum, coupled to the SM via the Z and Higgs portals. A ultraviolet (UV) completion of this model containing heavy vector-like fermions has been studied in previous literature. Here we construct and analyze for the first time a different UV completion of the model, which includes a dark Z' vector mixed with the Standard Model (SM) gauge bosons.

In chapter 1 we review the hierarchy problem, its symmetry-based solutions, and the essential features of NN models. In chapter 2 we introduce two theoretical tools, chiral perturbation theory (ChPT) and the electroweak precision tests (EWPT) of the SM, which prove indispensable in the later discussion. In chapter 3 we outline the properties of confining dark sectors inspired by NN, first starting with the well-known Fraternal Twin Higgs model, then moving on to the Z portal model that is the main focus of this thesis. We review the UV completion involving heavy fermions, and illustrate the application of ChPT to the calculation of dark pion decay rates.

Our original results are presented in chapter 4 and chapter 5. After writing down the Lagrangian of the Z' completion, we derive important bounds from EWPT and Z invisible decays. Then we calculate the effective decay constant of the CP -odd dark pions in terms of the underlying model parameters, comparing the results with those found previously in the completion containing heavy fermions. In addition, we discuss the decays of CP -even dark pions. These results will, hopefully, provide a basis for future phenomenological studies of the Z' model. In chapter 6 we offer our conclusions.

Chapter 1

Introduction

Thanks to the discovery of the Higgs boson back in 2012 [1, 2], one big unknown of the Standard Model (SM) has been revealed and our understanding of the fundamental building blocks of nature has deepened. The SM is a strong candidate for the most successful theory scientists have come up with thus far: under a radical reductionist point of view, *almost* all known phenomena in the whole Universe can be explained by the interactions that *particles* of the SM have among each other.

However, beneath this optimistic narration of our knowledge, there are several twists in the flow of reality that we have not understood yet. We observe phenomena that cannot be described only by the constituents of the SM: from gravity, to the accelerated expansion of the Universe (dark energy), but also Dark Matter (DM). Other pressing open problems include: neutrino masses [3, 4], the strong *CP* problem [5, 6], the matter/antimatter asymmetry [7, 8], and the hierarchy problem of the Higgs boson. Therefore, the SM is not enough and must be extended in order to explain such phenomena.

Actually, any theory can be thought as an effective theory of a bigger, more general one, as long as they both reproduce the same physical results under the same circumstances and with the right assumptions. These theories are related by a physical quantity, called *expansion parameter*, which regulates the range of validity of each one. For example, we can write the weight force acting on an object of mass m as

$$\vec{F}_g = -mg\hat{r}, \quad (1.1)$$

where $g = 9.81 \text{ m/s}^2$ is the acceleration of gravity and \hat{r} is the unit vector pointing away from the center of Earth. We could ask ourselves if this law is always valid or, for example, if we see a discrepancy as we increase our distance from the surface of the Earth. This is in fact the case, so we can assume that an extension to our theory that includes this effect must exist. We know that such a theory is Newton's theory of gravity; it states that the attractive force acting on an object of mass m dislocated by \vec{r} from an object with mass M is

$$\vec{F}_g = -G_N \frac{mM}{r^2} \hat{r}, \quad r \equiv |\vec{r}|, \quad (1.2)$$

where G_N is Newton's constant. Hence, we can think of Eq. (1.1) as the effective theory of Eq. (1.2) and the expansion parameter is the separation r . As long as r is close to the radius of Earth, then Eq. (1.1) holds, but if we increase the separation between an object and Earth, then we must resort to Eq. (1.2). Similarly, Newton's law of gravitation can be thought as the effective theory of Einstein's theory of General Relativity (GR). GR can also be ultimately regarded as the effective field theory (EFT) of its natural but yet unknown extension: quantum gravity.

Usually, in particle physics the expansion parameter is the ratio between the energy scale of the physical processes one is interested in, and the energy scale Λ (usually referred to as “cutoff”) where new degrees of freedom (i.e. particles) appear. Historically speaking, we have been able to observe new phenomena by increasing the energy at which particles are collided; in particular, new physical

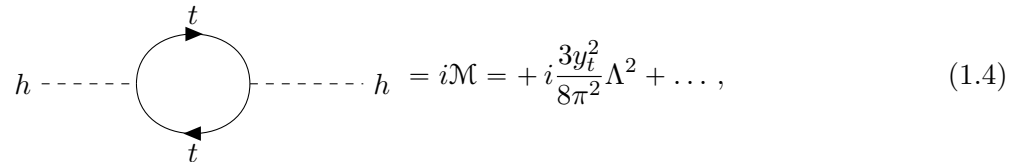
states can be produced and directly detected. What can be the natural cutoff of the SM? We know that gravity effects become non-negligible at the Planck scale $M_P \approx 10^{18}$ GeV, suggesting that also the SM is an EFT of a more fundamental theory that includes quantum gravity.

Even without invoking quantum gravity, it is possible to argue that the SM is not consistent within itself in the deep ultraviolet (UV) and requires a completion [9]. Hence, it necessarily has to be regarded as an EFT. We know the value at the Z pole of the measured hypercharge coupling $\alpha_1 = g_1^2/(4\pi)$, where $g_1 \equiv \sqrt{5/3}g'$ is the usual normalization adopted in Grand Unified Theories. We also know the expression of the β -function of α_1 , which at one loop is

$$\frac{d\alpha_1}{d \log \mu} = \frac{41}{10} \frac{\alpha_1^2}{2\pi}, \quad (1.3)$$

so by running α_1 to higher energies we find that it reaches a Landau pole at $\sim 10^{41}$ GeV. This suggests that the SM is UV-flawed and naturally requires an extension.

Among the aforementioned open questions, in this thesis we focus on the hierarchy problem and (some of) its possible solutions. We introduce a series of motivated models and explore their phenomenological consequences. The starting point is to ask ourselves what exactly the hierarchy problem is. Usually, it is introduced by considering the leading quantum corrections to the Higgs mass in the SM, which at 1-loop are mostly due to the top quark loop diagram



$$h \text{ --- } \text{loop} \text{ --- } h = i\mathcal{M} = +i\frac{3y_t^2}{8\pi^2}\Lambda^2 + \dots, \quad (1.4)$$

where the dots represent sub-leading corrections in the UV cutoff Λ . It is clear that if we push Λ to big values, such as for instance the Planck scale M_P , then the one loop correction needs to be finely tuned to an enormous level of precision, so that the physical squared mass of the Higgs matches the experimental value. This certainly appears unnatural.

Naively, one could be tempted to argue that the above effect is related to the way we chose to deal with divergences in quantum field theory, and is not physical. For example, we could work in dimensional regularization, parameterize our divergences in terms of $1/\epsilon$ and reabsorb them with the \overline{MS} scheme. However, the meaning of Eq. (1.4) is far deeper: there, Λ really serves as a proxy for the mass scale(s) of the UV completion, to which the Higgs mass is highly sensitive. In fact, we are soon going to introduce concrete models of new physics where the quadratic Λ^2 corrections to the Higgs mass are removed, and the cutoff is replaced by the physical masses of the new particles. These models are often referred to as “symmetry-based solutions” of the hierarchy problem.

Assuming this interpretation, we can estimate the energy scale where new particles should appear for the Higgs mass to be natural, namely, to avoid the necessity for fine tuning. Requiring the radiative correction to be smaller than the physical Higgs mass we obtain

$$m_{h,\text{phys}}^2 \gtrsim \frac{3y_t^2}{4\pi^2}\Lambda^2 \quad (1.5)$$

which translates, given that $m_{h,\text{phys}} \approx 125$ GeV, into

$$\Lambda \lesssim \sqrt{\frac{4\pi^2}{3y_t^2}} m_{h,\text{phys}} \approx 500 \text{ GeV}. \quad (1.6)$$

This means that for the Higgs mass to be fully natural, we expect new physics to appear at or below 500 GeV. A moderate amount of cancellation could be present in the theory, and allowing for – say – a tuning of 10%, the expectation for the scale of new physics relaxes to $\Lambda \lesssim 1.5$ TeV. Even in such

less strict version, this expectation from naturalness provides a very strong motivation to searches for new particles at colliders. Historically, this has been the key driver of the LHC physics programme.

Before moving on to introduce the symmetry-based solutions, we note briefly that the naturalness criterion has showed its strength in the past. The most notable example dates back to 1974 and the prediction of the charm quark by Gaillard and Lee [10]. In a theory with only up, down and strange quarks, the mass splitting between the K_L and K_S is quadratically divergent:

$$\frac{m_{K_L} - m_{K_S}}{m_{K_L}} \sim \frac{G_F^2 f_K^2}{16\pi^2} \sin^2 \theta_C \cos^2 \theta_C \Lambda^2, \quad (1.7)$$

with $f_K = 114$ MeV being the kaon decay constant and θ_C the Cabibbo mixing angle. Imposing that the correction is smaller than the experimental value gives $\Lambda < 2$ GeV. The divergence is cancelled if we include in our computation the fourth type of quark, the charm, with the effect of replacing $\Lambda \rightarrow m_c$. The experimental value of the charm mass, $m_c = 1.3$ GeV, turns out to be perfectly consistent with the naturalness criterion. Another well-known example is the mass difference between the charged and neutral pions, which dominantly originates from electromagnetic effects cut off at $\Lambda \sim m_\rho$, the mass of the ρ meson [11].

1.1 Symmetry-based solutions of the hierarchy problem

We now turn to the theoretical constructions that address the largest quantum correction to the Higgs mass in the SM, originating from the interaction with the top quark, see Eq. (1.4). We are going to introduce only the minimal ingredients required to understand how these models achieve a cancellation in the largest, quadratic corrections to the mass of the Higgs.

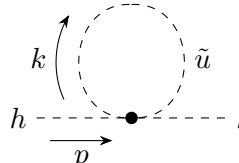
The first example is given by super-symmetry (SUSY), see e.g. Ref. [12] for a pedagogical introduction. We add to the SM *two complex scalar fields*, $\tilde{u}^c \sim (\mathbf{\bar{3}}, \mathbf{1})_{-2/3}$ and $\tilde{q} = (\tilde{u} \ \tilde{d})^T \sim (\mathbf{3}, \mathbf{2})_{1/6}$ under $SU(3)_c \times SU(2)_L \times U(1)_Y$. These fields play the role of the top superpartners and have the following Lagrangian

$$\mathcal{L} = -y_t \bar{q}_L \tilde{H} t_R + \text{h.c.} - y_t^2 |\tilde{u}^c|^2 |H|^2 - y_t^2 |\tilde{q} H|^2, \quad (1.8)$$

where $\tilde{H} \equiv i\sigma_2 H^*$ and $\tilde{q} H = (\tilde{u} \ \tilde{d}) i\sigma_2 (H^+, H^0)^T$. By expanding the Higgs doublet in unitary gauge, i.e. $H = (0, h/\sqrt{2})^T$ with h being the Higgs boson, we obtain the following interaction term

$$\mathcal{L} \supset -y_t^2 |\tilde{u}|^2 \frac{h^2}{2} - (\tilde{u} \leftrightarrow \tilde{u}^c). \quad (1.9)$$

The contribution to the Higgs self-energy can then be written, neglecting the masses of the new fields in first approximation, as



$$\begin{aligned} &= i\mathcal{M} = -iN_c y_t^2 \int \frac{d^4 k}{(2\pi)^4} \frac{i}{k^2} \stackrel{k^0 \mapsto i k_E^0}{=} -iN_c y_t^2 \int \frac{d^4 k_E}{(2\pi)^4} \frac{1}{k_E^2} \\ &= -\frac{iN_c y_t^2}{(2\pi)^4} \int \underbrace{d\Omega_4}_{2\pi^2} \int_0^\Lambda dk_E k_E \stackrel{N_c=3}{=} -i \frac{3y_t^2}{8\pi^2} \frac{\Lambda^2}{2}. \end{aligned} \quad (1.10)$$

From \tilde{u}^c we get an identical correction which, summed with Eq. (1.10), exactly cancels Eq. (1.4).

A different way of cancelling the Higgs quadratic divergences is by introducing *vector-like fermions* as partners of the top quark. These are fermions whose left and right-handed components have the

same quantum numbers under the SM. By adding to the SM a new field $T \sim (\mathbf{3}, \mathbf{1})_{2/3}$ and write the relevant pieces of the Lagrangian as

$$\mathcal{L} = -y_t \bar{q}_L \tilde{H} t_R + \text{h.c.} + y_t \bar{T} T \frac{|H|^2}{2f} - y_t f \bar{T} T. \quad (1.11)$$

This is a proxy for Little Higgs [13] and, more generally, composite Higgs [14] scenarios (though in the latter case, the role that here is played by T is shared by multiple states). Now f has the dimension of a vacuum expectation value (vev), distinct from the Higgs vev $v \approx 246.2$ GeV. By expanding $H = (0, h/\sqrt{2})^T$ this Lagrangian produces the following interaction

$$= +i \frac{y_t}{2f}$$

Hence we can draw the correction to the Higgs mass (notice that in this case we must retain the mass of the new particle, $m_T = y_t f$, in the calculation)

$$h \text{ --- } \bullet \text{ --- } h = i\mathcal{M} = +i \frac{y_t}{2f} N_c(-1) \int \frac{d^4 k}{(2\pi)^4} \text{Tr} \left[\frac{i}{\not{k} - m_T} \right] = \dots \quad (1.12)$$

$$= -i \frac{3y_t^2}{8\pi^2} \Lambda^2 + \dots,$$

where the dots in the second line indicate terms that are subleading for large Λ . We see that this exactly cancels the quadratic divergence induced by the top loop, Eq. (1.4).

1.2 Changing perspective: Neutral Naturalness, and the Twin Higgs

While extremely simplified, the models described above capture the leading ingredients used to address the hierarchy problem using continuous symmetries, namely either a spacetime symmetry (SUSY), or a global symmetry (Higgs as a pseudo-Goldstone boson, characteristic of Little Higgs/Composite Higgs scenarios). The common prediction of these models is the presence of relatively light top partner states, either scalar or fermionic, which are charged under SM QCD. These states must be relatively light because, although the quadratically divergent Λ^2 terms are absent from the theory, analogous radiative corrections exist where Λ is replaced by the masses of the new particles.

QCD-charged particles are produced with sizeable rates at the LHC, but so far the search for their signals has been unsuccessful. The bounds on these partners have become tighter after Run 1 and Run 2 of LHC. In particular, as shown in Fig. 1.1, the mass of the stop (SUSY top partner) must lie above approximately 1.2 TeV for most values of the neutralino mass. New vector-like quarks are similarly constrained: as shown in Fig. 1.2, fermionic top partners need to be heavier than 1.4 to 1.6 TeV. These experimental results cast doubt about the plausibility of these “classic” models for Higgs naturalness, and call for different approaches to the problem.

An alternative way to enforce Higgs naturalness, which serves as important inspiration for this thesis, is to make use of discrete (rather than continuous) symmetries. These discrete symmetries relate the SM to a new sector of particles, which is endowed with its own gauge interactions but is *neutral* under the SM gauge group. For this reason, these type of solutions go under the name of *Neutral Naturalness* (NN) models. They represent a more recent development in the area of symmetry-based

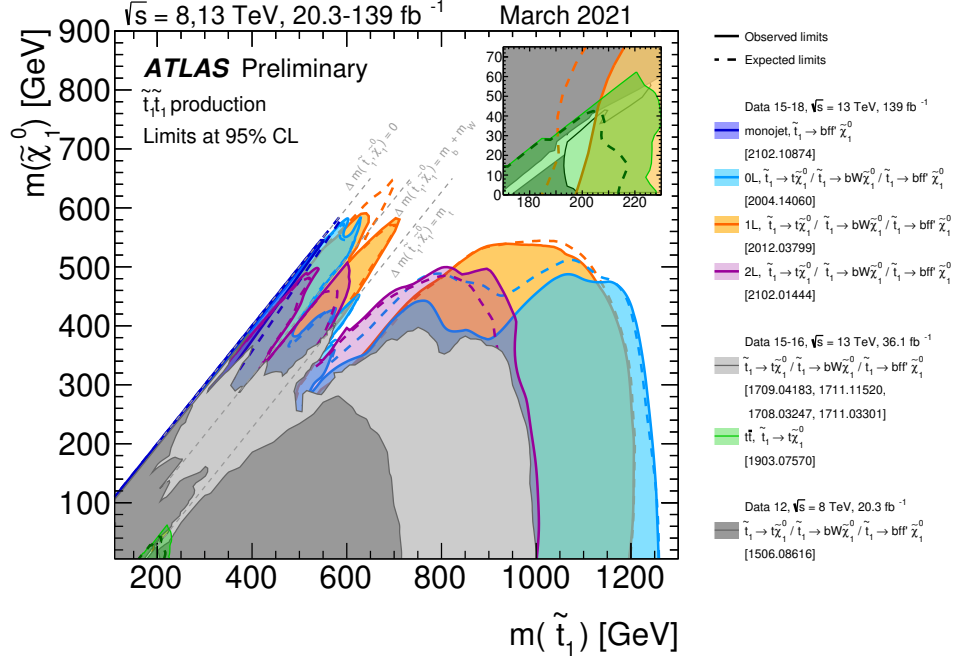


Figure 1.1: Stop-neutralino mass plane showing the exclusion limits according to the latest results of the ATLAS experiment at the LHC [15]: the solid (dashed) lines represent the measured (expected) boundaries. In models with light neutralino $\tilde{\chi}_1^0$, the stop must be heavier than about 1.2 TeV.

solutions to the hierarchy problem. While their origin dates back to the mid-2000s, with the seminal papers by Chacko, Harnik, and others [17, 18], a more systematic analysis of NN models has been undertaken only from ~ 2015 onwards [19–29] and their study is still ongoing, especially as far as the experimental signatures are concerned [30–34]. The phenomenology of NN is, in fact, strikingly different from classic QCD-charged naturalness, as it will be discussed at length in this thesis.

We now introduce the Twin Higgs models [17], which constitute the best-studied incarnation of NN. In these theories the Higgs boson is described as a pseudo Nambu-Goldstone particle (pNGB) associated to the spontaneous breaking at scale f of an extended global symmetry. Minimally, a global $SU(4)$ is broken to $SU(3)$, giving rise to 7 Goldstone bosons. Among these 7 degrees of freedom, four make up the SM-like Higgs doublet, whereas three are eaten to become the longitudinal components of the \hat{W} and \hat{Z} bosons in the Twin sector (in this chapter we denote Twin fields with a hat). As it will become clear momentarily, the key ingredient is a \mathbb{Z}_2 symmetry that exchanges the SM and Twin sectors. This \mathbb{Z}_2 enhances the symmetry of the quadratically divergent part of the radiative Higgs potential, thus removing the largest impediment to Higgs naturalness. The Twin sector is neutral under all SM gauge symmetries, including the top partner \hat{t} , which cancels the quadratic divergence through the same mechanism shown in Eq. (1.12). The needed color factor arises from $N_d = 3$, where $SU(N_d)$ is the Twin color group, distinct from the SM color group.

We focus on a minimal version of the Twin Higgs where only the fields that are strictly necessary to solve the hierarchy problem are introduced. The model is known as “Fraternal” Twin Higgs [21]. Suppose to have a complex scalar \mathcal{H} transforming in the fundamental representation of an $SU(4)$ global symmetry, with potential

$$V = \lambda \left(|\mathcal{H}|^2 - \frac{f^2}{2} \right)^2 \quad (1.13)$$

such that the vev of $\langle \mathcal{H} \rangle$ breaks the symmetry $SU(4) \rightarrow SU(3)$. Out of the 7 resulting pNGBs, one will be identified with the physical Higgs boson h . The gauge and Yukawa interactions break explicitly the $SU(4)$ symmetry, under which the SM fields (labeled A) and Twin fields (labeled B) do not form complete representations. However, they are related by a \mathbb{Z}_2 exchange symmetry $A \leftrightarrow B$. In

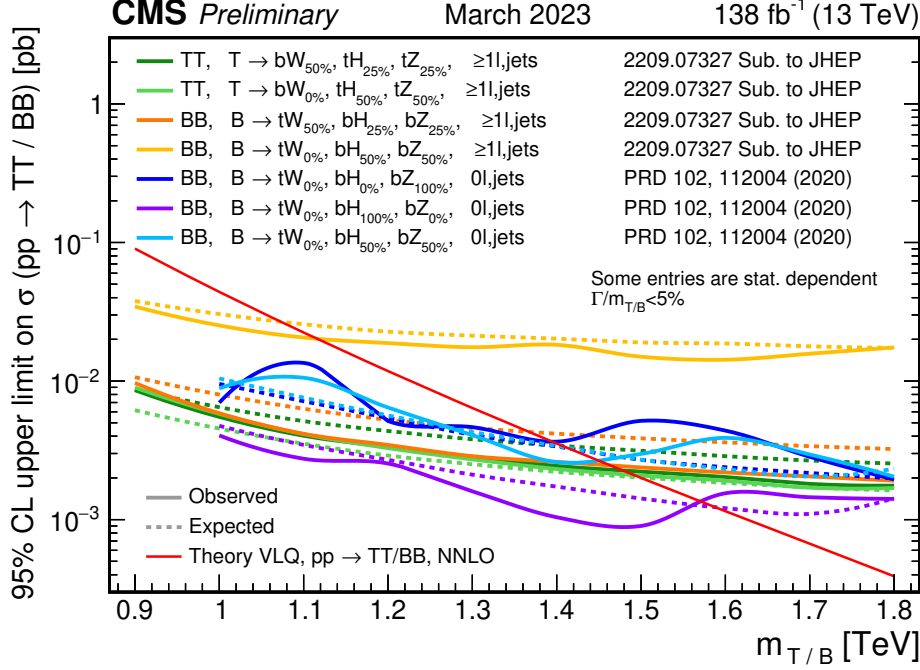


Figure 1.2: Observed (solid) and expected (dashed) 95% CL upper limits on the production cross section of pairs of vector-like quarks (\overline{TT} or \overline{BB}) as a versus their masses, as obtained by different analyses performed by the CMS experiment at the LHC. Figure taken from Ref. [16].

fact we can decompose the full scalar multiplet as $\mathcal{H} = (A, B)$, where A indicates the Higgs doublet (with the identifications $SU(2)_A = SU(2)_L$ and $A = H$, in the conventional notation) and B is a new doublet, charged under the Twin weak interaction $SU(2)_B$. Once the SM and Twin weak interactions are gauged and the exchange symmetry is imposed, the quadratically divergent contributions to the Higgs mass coming from the gauge loops cancel. To see this, recall the situation in the SM, where the following diagrams

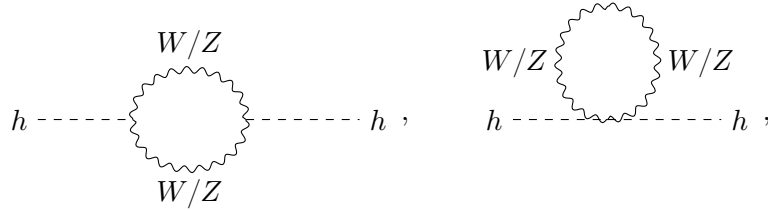


Figure 1.3: Quadratically divergent contributions to the Higgs mass from SM gauge boson loops.

produce a $\sim (400\text{GeV})^2$ contribution to the Higgs squared mass for a UV cutoff $\Lambda = 5\text{ TeV}$. In the Twin Higgs model, each of A and B receives this type of 1-loop quadratic corrections:

$$V_{1\text{-loop}} = \frac{9g_2^2\Lambda^2}{64\pi^2}|A|^2 + \frac{9\hat{g}_2^2\Lambda^2}{64\pi^2}|B|^2 + \dots \quad (1.14)$$

Crucially, if we enforce the \mathbb{Z}_2 symmetry then it follows that $g_2 = \hat{g}_2$ (at the high scale Λ), so that Eq. (1.14) will take the form

$$V_{1\text{-loop}} = \frac{9g_2^2\Lambda^2}{64\pi^2}|\mathcal{H}|^2 + \dots \quad (1.15)$$

which is accidentally $SU(4)$ invariant. This means that the pNGB masses are insensitive to quadratic corrections arising from gauge loops. On the other hand, even in the \mathbb{Z}_2 symmetric limit the gauging

produces logarithmically divergent corrections to the pNGB masses,

$$\Delta V_{1\text{-loop}} \propto \frac{g_2^4}{16\pi^2} \log\left(\frac{\Lambda}{g_2 f}\right) (|A|^4 + |B|^4), \quad (1.16)$$

but these do not pose a problem from a naturalness standpoint up to $\Lambda \lesssim 4\pi f$, the scale where a UV completion of Twin Higgs must eventually kick in. We can therefore say that the Twin Higgs is a solution to the *little* hierarchy problem, effective up to a scale Λ in the range from 5 to 10 TeV.

In fact, the logarithmic divergences in Eq. (1.16) could be removed as well, by extending the SM and Twin sectors to complete multiplets of $SU(6) \times SU(4)$, where the SM and Twin color groups are embedded in the $SU(6)$ [17]. This implies the appearance of new states with gauge charges under both sectors and masses in the multi-TeV range, with exotic phenomenology [26]. However, here we do not attempt such extension, limiting ourselves to a simpler description where logarithmic divergences are present but not dangerous.

The gauging of Twin hypercharge is not necessary to solve the little hierarchy problem, although it is possible to include it [17]. For simplicity, here we assume that Twin hypercharge is a global symmetry, or a gauge symmetry broken at the scale Λ .

Let us now discuss the biggest radiative corrections to the Higgs mass, arising from the top Yukawa coupling. We introduce a Twin left-handed fermion doublet, \hat{Q}^a , transforming under $SU(2)_B$, as well as a Twin right-handed singlet fermion \hat{u}^a . Here, a is an index of the Twin color group. These fermions couple to the B doublet as

$$\mathcal{L} \supset -\hat{y}_t \hat{Q} B \hat{u}. \quad (1.17)$$

We will soon argue that the Twin color symmetry should be gauged, although at the level of the present (1-loop) argument it might as well be a global symmetry. The 1-loop corrections to the scalar potential coming from the top quark and its Twin can be written as

$$16\pi^2 V_{1\text{-loop}} = -6y_t^2 \Lambda^2 |A|^2 - 6\hat{y}_t^2 \Lambda^2 |B|^2 + 3y_t^4 |A|^4 \log\left(\frac{\Lambda^2}{y_t^2 |A|^2}\right) + 3\hat{y}_t^4 |B|^4 \log\left(\frac{\Lambda^2}{\hat{y}_t^2 |B|^2}\right). \quad (1.18)$$

The magic of Twin Higgs manifests again: as long as the \mathbb{Z}_2 enforces $y_t = \hat{y}_t$ at high scale Λ , the quadratic corrections arrange into an accidentally $SU(4)$ invariant structure. The logarithmic corrections remain, and constitute an important but acceptable contribution to the potential of the SM-like Higgs.

A smaller, but still relevant, correction to the Higgs mass arises at two loops, from QCD corrections. Although the gluons do not couple directly to the Higgs, they do couple to the top and at 2-loop order they contribute about $\sim (350\text{GeV})^2$ to the Higgs mass squared, for a cutoff of 5 TeV. In order to cancel this contribution we gauge the Twin QCD, obtaining

$$(\delta m_h^2)_{2\text{-loop}} \approx \frac{3y_t^2 \Lambda^2}{4\pi^4} (g_s^2 - \hat{g}_s^2). \quad (1.19)$$

Again, requiring \hat{g}_s to be (approximately) equal to the SM QCD coupling g_s at the UV scale Λ removes this quadratic correction, allowing for a fully natural Higgs mass. We will return to this aspect in the next section.

In the Fraternal Twin Higgs model a right-handed Twin bottom quark \hat{b} is also present, in order to cancel anomalies. It couples to the B doublet via

$$\mathcal{L} \supset -\hat{y}_b \hat{Q} B \hat{b}. \quad (1.20)$$

Here the \mathbb{Z}_2 symmetry does not need to be enforced, but to avoid introducing a new hierarchy problem we still require $\hat{y}_b \ll y_t$. In the same fashion, a Twin lepton doublet \hat{L} and right-handed Twin tau $\hat{\tau}$ are included for anomaly cancellation. Twin fermions of the first two generations are not needed for Higgs naturalness and are therefore left out of the Fraternal model.

Another important concept to mention is the so-called “vacuum alignment”. The vev that breaks the global $SU(4)$ can be decomposed as

$$f^2 = v_A^2 + v_B^2. \quad (1.21)$$

As we already mentioned, 6 pNGBs are eaten up in the spontaneous breakdown of the SM and Twin electroweak symmetries, leaving as physical scalar degrees of freedom a single pNGB, eventually associated with the SM-like Higgs boson, and the heavy radial mode of the linear sigma model. An exact \mathbb{Z}_2 would imply $v_A = v_B$, leading to the physical Higgs being an equal mixture of A and B , which is not compatible with Higgs couplings data since only A carries SM quantum numbers. Therefore, a phenomenologically viable realization requires $v_A \ll v_B$, by a factor of a few. This means that the \mathbb{Z}_2 must be broken, either spontaneously or explicitly, to some extent. Many possible sources of this breaking have been considered in the literature; see for example Ref. [35] for recent developments.

1.3 The motivation for confinement in the dark sector

In the discussion around Eq. (1.19) we have argued that Twin color should be promoted to a gauge symmetry, in order to cancel the 2-loop quadratic divergences arising from diagrams involving SM top and gluon lines. The coupling of Twin QCD should be approximately equal to g_s at the scale Λ , leading to Twin confinement at low energies. This is a general aspect of NN models, essentially all of which predict that the dark sector confines at a scale not far from the GeV. Given the centrality of this statement for our work – which focuses on dark hadron phenomenology – here we discuss the motivation for dark confinement in greater detail, taking again the Fraternal Twin Higgs as our working example [21].

At one loop, the renormalization group equations for the SM and Twin couplings can be written as

$$\frac{dy_t}{d \log \mu} = \frac{9y_t^3}{32\pi^2} - \frac{y_t g_s^2}{2\pi^2}; \quad \frac{d\hat{y}_t}{d \log \mu} = \frac{9\hat{y}_t^3}{32\pi^2} - \frac{\hat{y}_t \hat{g}_s^2}{2\pi^2} \quad (1.22)$$

$$\frac{dg_s}{d \log \mu} = -\frac{7g_s^3}{16\pi^2}; \quad \frac{d\hat{g}_s}{d \log \mu} = -\frac{29\hat{g}_s^3}{48\pi^2}, \quad (1.23)$$

whereas the running of the Higgs mass, defining $x \equiv m_h^2(\mu)/\mu^2$, is given by

$$\frac{dx}{d \log \mu} = -2x + \frac{3(\hat{y}_t^2 - y_t^2)}{2\pi^2}. \quad (1.24)$$

Suppose now that $\hat{g}_s = 0$. Neglecting the running of g_s in first approximation, we solve the above equations for y_t and \hat{y}_t and feed the results into Eq. (1.24), obtaining

$$m_h^2(\mu) \approx m_h^2(\Lambda) + \left[\frac{3y_t^2 g_s^2}{8\pi^4} + \frac{3(y_t^2 - \hat{y}_t^2)}{4\pi^2} \right] (\Lambda^2 - \mu^2) - \frac{3y_t^2 g_s^2}{8\pi^4} \mu^2 \log \left(\frac{\Lambda}{\mu} \right), \quad (1.25)$$

which in the IR limit $\mu_{\text{IR}} \ll \Lambda$ is

$$m_h^2(\mu_{\text{IR}}) \approx m_h^2(\Lambda) + \left[\frac{3y_t^2 g_s^2(\Lambda)}{8\pi^4} + \frac{3(y_t^2 - \hat{y}_t^2)(\Lambda)}{4\pi^2} \right] \Lambda^2. \quad (1.26)$$

Thus, even if $y_t = \hat{y}_t$ at the UV scale Λ , the running of SM QCD has produced a quadratic divergence in the Higgs mass. This requires a fine tuning

$$\frac{m_{h,\text{phys}}^2}{\frac{3y_t^2(\Lambda)g_s^2(\Lambda)}{8\pi^4}\Lambda^2} \approx 0.25, \quad (1.27)$$

if the UV cutoff is set to $\Lambda = 5$ TeV for concreteness. The effect can be significantly mitigated if Twin QCD is gauged. In this case Eq. (1.26) becomes

$$m_h^2(\mu_{\text{IR}}) \approx m_h^2(\Lambda) + \left[\frac{3y_t^2(g_s^2 - \hat{g}_s^2)(\Lambda)}{8\pi^4} + \frac{3(y_t^2 - \hat{y}_t^2)(\Lambda)}{4\pi^2} \right] \Lambda^2. \quad (1.28)$$

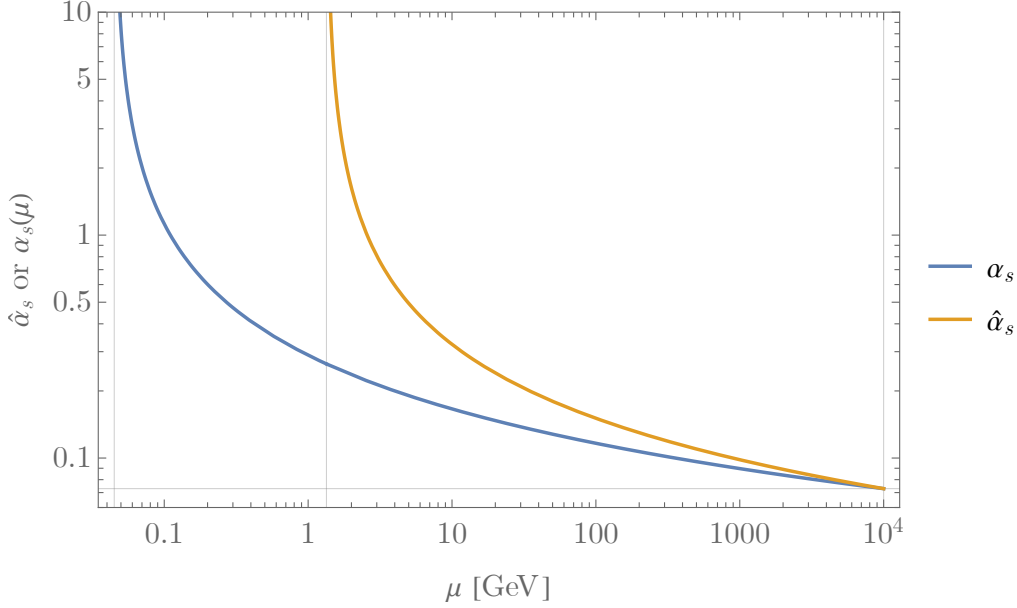


Figure 1.4: Running of the QCD and Twin QCD coupling constants in the Fraternal Twin Higgs model. We have set $\alpha_s(\Lambda) = 0.073$ with $\Lambda = 10$ TeV. Note how $\hat{\alpha}_s$ has a bigger confinement scale, $\hat{\Lambda}_{\text{QCD}} > \Lambda_{\text{QCD}}$.

Hence, even approximate equality of g_s and \hat{g}_s at scale Λ essentially removes this 2-loop source of fine tuning.

Finally, given $g_s(\Lambda) \approx \hat{g}_s(\Lambda)$ we can ask about the confinement scale of Twin QCD. The β -functions in Eq. (1.23) only differ because the SM and Twin sectors contain different numbers of quarks. We write, taking for instance SM QCD,

$$\frac{d\alpha_s}{d \log \mu} = -\frac{7\alpha_s^2}{2\pi}, \quad (1.29)$$

where $\alpha_s = g_s^2/(4\pi)$, obtaining for the solutions

$$\alpha_s(\mu) = \frac{\alpha_s(\Lambda)}{1 - 7 \frac{\alpha_s(\Lambda)}{2\pi} \log(\Lambda/\mu)}, \quad \hat{\alpha}_s(\mu) = \frac{\hat{\alpha}_s(\Lambda)}{1 - \frac{29}{3} \frac{\hat{\alpha}_s(\Lambda)}{2\pi} \log(\Lambda/\mu)}. \quad (1.30)$$

We know that $\alpha_s(M_Z) \approx 0.118$ [36], so we run α_s up to Λ (fixed to 10 TeV for the sake of example), obtaining $\alpha_s(\Lambda) \approx 0.073$. Then we impose the condition $\alpha_s(\Lambda) = \hat{\alpha}_s(\Lambda)$ and run $\hat{\alpha}_s$ down to the infrared. The results are shown in Fig. 1.4, where we find that the confinement scale of Twin QCD is approximately one order of magnitude larger than for SM QCD. This is a model-specific result, which follows from the minimal Twin quark content of the Fraternal model; the general lesson is that indeed the dark and SM QCD dynamics confine at comparable scales. We should also mention that the above calculation is extremely simplified, being limited to 1-loop running of the couplings and neglecting threshold corrections. Nevertheless, the qualitative conclusions hold even when a more accurate analysis is performed.

1.4 Summary: particle content of the Fraternal Twin Higgs

To conclude our Introduction, we summarize the particle content of the Fraternal Twin Higgs model. Although in the remainder of this thesis we will not focus specifically on this model, several features are general in NN models and provide important inspiration for the original work presented in chapters 4 and 5. The key features are:

1. A Twin Higgs doublet B , combined with the SM doublet A into \mathcal{H} with $SU(4)$ -invariant potential;

2. A Twin electroweak group $SU(2)_B$, whose gauge coupling is approximately equal to the one of the SM at the UV scale $\Lambda \sim 5$ to 10 TeV;
3. A Twin top, with Twin top Yukawa that is approximately equal to the one of the SM top at Λ ;
4. Twin gluons, responsible for improving Higgs naturalness at the 2-loop level;
5. Additional fields (twin bottom, twin tau, twin neutrinos) which are required for consistency of the theory, but do not play a role in protecting the Higgs mass.

We stress once more that this is the minimal particle content of the theory. Many extensions and variations have been considered in the literature. One important aspect is that the Fraternal Twin Higgs is cosmologically safe, whereas “mirror” models where all SM fields have a Twin counterpart predict an excessively large number of relativistic degrees of freedom and clash with Cosmic Microwave Background observations. Nevertheless, solutions to this well-known problem exist [37].

Having completed our first encounter with NN models, in chapter 3 we will turn to the phenomenology of their confining dark sectors, which are a rather universal feature of this type of approach to the little hierarchy problem. Before we do that, however, we will spend chapter 2 building some useful theoretical tools.

Chapter 2

Some theoretical tools

Before continuing our discussion of strongly-interacting dark sectors, which are the main focus of this thesis, we dedicate this chapter to two theoretical tools that will prove indispensable. The first one is chiral perturbation theory and the second one is the treatment of electroweak precision tests of the SM.

2.1 Chiral perturbation theory (ChPT)

QCD is the accepted theory of the strong interactions. It is asymptotically free, hence perturbative calculations are only possible at large momentum transfer. Conversely, QCD becomes strongly coupled in the infrared, with $\Lambda_{\text{QCD}} \approx 200$ MeV. Here lattice calculations are in general required, at large computational cost. However, if we focus on the dynamics of the lightest degrees of freedom – the pseudoscalar meson octet – then it is possible to construct ChPT, an effective theory that exploits the chiral symmetries of the QCD Lagrangian and their systematically controlled breaking. In this EFT, the lightest pseudoscalar mesons are described as pNGBs. Many excellent reviews of and introductions to ChPT exist [38, 39].

The mass spectrum of the SM quarks spans several orders of magnitude, from 2.2 MeV for the up quark to 173 GeV for the top [36]. Crucially, three of the quarks are lighter than the confinement scale of QCD.

m_u	m_d	m_s	m_c	m_b	m_t
2.2 MeV	4.7 MeV	93 MeV	1.3 GeV	4.2 GeV	173 GeV
lighter than Λ_{QCD}			heavier than Λ_{QCD}		

We now consider only the u, d, s . The QCD Lagrangian can be written as

$$\mathcal{L}_{\text{QCD}} = -\frac{1}{4}G_{\mu\nu}^A G^{\mu\nu,A} + (\bar{q}_L i \not{D} q_L + \bar{q}_R i \not{D} q_R) - \bar{q}_L M q_R + \text{h.c.} \quad (2.1)$$

with

$$D_\mu = \partial_\mu - i g_s T^A G_\mu^A, \quad M = \text{diag}(m_u, m_d, m_s), \quad \text{and} \quad q = \begin{pmatrix} u \\ d \\ s \end{pmatrix}. \quad (2.2)$$

Here A is a color index. The kinetic part of the Lagrangian is invariant under a global $SU(3)_L \times SU(3)_R \times U(1)_V$. The quarks transform as follows under the $SU(3)_{L,R}$,

$$\begin{cases} q_L \mapsto L q_L \\ q_R \mapsto R q_R \end{cases}. \quad (2.3)$$

We observe that the mass term couples left- and right-handed fermions, hence breaking explicitly the chiral symmetry. In order to render the full Lagrangian formally invariant under chiral transforms, we promote the mass matrix to a spurion obeying $M \mapsto LMR^\dagger$.

The QCD vacuum breaks spontaneously the $SU(3)_L \times SU(3)_R \times U(1)_V$ symmetry down to $SU(3)_V \times U(1)_V$,

$$\langle 0 | \bar{q}_{R,j} q_{L,i} | 0 \rangle = \Lambda_{\text{QCD}}^3 \delta_{ij} \quad (2.4)$$

where i, j are generation indices. Transforming the quarks according to Eq. (2.3), we obtain

$$\langle 0 | \bar{q}_{R,j} q_{L,i} | 0 \rangle \mapsto \langle 0 | \bar{q}_{R,j} q_{L,i} | 0 \rangle R_{qj}^\dagger L_{iq} = \Lambda_{\text{QCD}}^3 \underbrace{(LR^\dagger)_{ij}}_{\Sigma_{ij}}. \quad (2.5)$$

We see that the vacuum condensate is invariant only if $L = R$, which means that the symmetry group is now reduced to $SU(3)_V$. The number of broken generators is 8, leading to 8 Goldstone bosons according to Goldstone's theorem. The situation is qualitatively similar when at least two light flavors are present; the case of only one light flavor is special, as already mentioned, since no Goldstone bosons are expected. The pNGBs are described by promoting Σ to a field,

$$\Sigma = \exp \left(2i \frac{\pi_a T^a}{f} \right), \quad (2.6)$$

that transforms chirally as $\Sigma \mapsto L \Sigma R^\dagger$. The π_a are the 8 pNGBs and the T^a are the broken $SU(3)$ generators, whereas f is identified at leading order with the pion decay constant,

$$\langle 0 | j_{5a}^\mu(0) | \pi_b(p) \rangle = -i \delta_{ab} f_\pi p^\mu, \quad j_{5a}^\mu = \bar{q} \gamma^\mu \gamma_5 T^a q, \quad (2.7)$$

normalized to $f_\pi \approx 93$ MeV.

We now write the first terms of the chiral Lagrangian, starting with the chirally invariant ones. At the two-derivative level we have

$$\mathcal{L}_2 = \frac{f_\pi^2}{4} \text{Tr}[(\partial_\mu \Sigma)^\dagger (\partial^\mu \Sigma)], \quad (2.8)$$

while the mass term is (imposing conservation of parity)

$$\mathcal{L}_M = \frac{B_0 f_\pi^2}{2} \text{Tr}[\Sigma M^\dagger + M \Sigma^\dagger]. \quad (2.9)$$

It can be shown that the new parameter B_0 is related to the vacuum condensate as $B_0 f_\pi^2 = -\langle 0 | \bar{q}_i q_i | 0 \rangle$.

In addition to the 8 pNGBs in our description we retain also the η' meson, which is not a Goldstone at finite N_c due to the $U(1)_A$ anomaly.¹ The Lagrangian then reads

$$\mathcal{L} = \frac{f_\pi^2}{4} \text{Tr}[(\partial_\mu \Sigma)^\dagger (\partial^\mu \Sigma)] + \frac{B_0 f_\pi^2}{2} \text{Tr}[\Sigma M^\dagger + M \Sigma^\dagger] - \frac{1}{2} m_0^2 \eta_0^2. \quad (2.10)$$

The explicit form of Σ is

$$\Sigma = \exp(2i\mathbf{P}/f_\pi), \quad \mathbf{P} = \frac{1}{\sqrt{2}} \begin{pmatrix} \frac{\pi_0}{\sqrt{2}} + \frac{\eta_8}{\sqrt{6}} + \frac{\eta_0}{\sqrt{3}} & \pi^+ & K^+ \\ \pi^- & -\frac{\pi_0}{\sqrt{2}} + \frac{\eta_8}{\sqrt{6}} + \frac{\eta_0}{\sqrt{3}} & K^0 \\ K^- & \bar{K}^0 & -\sqrt{\frac{2}{3}} \eta_8 + \frac{\eta_0}{\sqrt{3}} \end{pmatrix}, \quad (2.11)$$

where $\mathbf{P} = \pi_a T^a + \eta_0 \mathbb{I}/\sqrt{6}$, with π_a ($a = 1, \dots, 8$) the pNGBs. For the masses of the complex pNGBs one finds readily

$$\begin{aligned} m_{\pi_\pm}^2 &= B_0(m_u + m_d), \\ m_{K_\pm}^2 &= B_0(m_u + m_s), \\ m_{K_0, \bar{K}_0}^2 &= B_0(m_d + m_s). \end{aligned} \quad (2.12)$$

¹It is known that including the η' and its mixing with η is important to obtain phenomenologically viable predictions for the $\eta, \eta' \rightarrow \gamma\gamma$ rates.

For simplicity, in this thesis we neglect the isospin breaking originating from $m_u \neq m_d$, which enters through the parameter

$$\delta_I \equiv \frac{m_d - m_u}{m_d + m_u} \approx \frac{1}{3}. \quad (2.13)$$

Neglecting isospin breaking implies that we do not have mixing between η_8 and π_0 . On the other hand, the mixing between η_8 and η_0 is found to be

$$\begin{aligned} & \frac{B_0 f_\pi^2}{2} \text{Tr}[\Sigma M^\dagger + M \Sigma^\dagger] - \frac{1}{2} m_0^2 \eta_0^2 \simeq -2B_0 \text{Tr}[\mathbf{P}^2 M] - \frac{1}{2} m_0^2 \eta_0^2 \\ & \supset -\frac{1}{2} \begin{pmatrix} \eta_8 & \eta_0 \end{pmatrix} \begin{pmatrix} \frac{2}{3} B_0 (m + 2m_s) & \frac{2\sqrt{2}}{3} B_0 (m - m_s) \\ \frac{2\sqrt{2}}{3} B_0 (m - m_s) & m_0^2 + \frac{2}{3} B_0 (m_s + 2m) \end{pmatrix} \begin{pmatrix} \eta_8 \\ \eta_0 \end{pmatrix}. \end{aligned} \quad (2.14)$$

The above matrix can be diagonalized via the rotation

$$\begin{pmatrix} \eta_8 \\ \eta_0 \end{pmatrix} = \begin{pmatrix} \cos \theta_{\eta\eta'} & \sin \theta_{\eta\eta'} \\ -\sin \theta_{\eta\eta'} & \cos \theta_{\eta\eta'} \end{pmatrix} \begin{pmatrix} \eta \\ \eta' \end{pmatrix}, \quad (2.15)$$

where η and η' are physical states, with

$$\tan \theta_{\eta\eta'} = \frac{\frac{2\sqrt{2}}{3} B_0 (m - m_s)}{m_{\eta'}^2 - \frac{2}{3} B_0 (m + 2m_s)} = \frac{-2\sqrt{2}(m_K^2 - m_\pi^2)}{3m_{\eta'}^2 - (4m_K^2 - m_\pi^2)}, \quad (2.16)$$

where we used the expressions of the masses for $\delta_I \rightarrow 0$,

$$m_\pi^2 = 2B_0 m, \quad m_K^2 = B_0 (m + m_s). \quad (2.17)$$

Since the physical mass of η' is $m_{\eta'} \approx 958$ MeV, we find that $\tan \theta_{\eta\eta'} \approx -0.353$ corresponding, to a good level of accuracy, to

$$\sin \theta_{\eta\eta'} \approx -\frac{1}{3}, \quad \cos \theta_{\eta\eta'} \approx \frac{2\sqrt{2}}{3}. \quad (2.18)$$

In the physical basis, the \mathbf{P} matrix takes the form

$$\mathbf{P} = \frac{1}{\sqrt{2}} \begin{pmatrix} \frac{\pi_0}{\sqrt{2}} + \frac{\eta}{\sqrt{3}} + \frac{\eta'}{\sqrt{6}} & \pi^+ & K^+ \\ \pi^- & -\frac{\pi_0}{\sqrt{2}} + \frac{\eta}{\sqrt{3}} + \frac{\eta'}{\sqrt{6}} & K^0 \\ K^- & \bar{K}^0 & -\frac{\eta}{\sqrt{3}} + \frac{2\eta'}{\sqrt{6}} \end{pmatrix}. \quad (2.19)$$

2.1.1 Couplings to photons and axion-like particles

Some of the pseudoscalar mesons are charged under electromagnetism (EM), so we now want to include in ChPT the effects of interactions with the photons. In order to do so, we write the current the photon couples to at quark level as

$$j_V^\mu = \bar{q}_L \gamma^\mu \mathbf{Q}_L q_L + \bar{q}_R \gamma^\mu \mathbf{Q}_R q_R, \quad \mathbf{Q}_L = \mathbf{Q}_R = \mathbf{Q}, \quad (2.20)$$

where $\mathbf{Q} = (2/3, -1/3, -1/3)$, implying that we can incorporate the effects of EM into a covariant derivative acting on the Σ field,

$$D_\mu \Sigma = \partial_\mu \Sigma - ie A_\mu \mathbf{Q}_L \Sigma + ie A_\mu \Sigma \mathbf{Q}_R = \partial_\mu \Sigma - ie A_\mu [\mathbf{Q}, \Sigma]. \quad (2.21)$$

Suppose now that an axion-like particle (ALP) is coupled to an axial current made out of quarks, as we are going to see in Eq. (3.12),

$$j_A^\mu = \bar{q} \gamma^\mu \gamma_5 \mathbf{c}_q q, \quad (2.22)$$

where $\mathbf{c}_q = \text{diag}(c_u, c_d, c_s)$. Again we are able to write a covariant derivative that includes the coupling of the ALP to the pNGBs,

$$D_\mu \Sigma = \partial_\mu \Sigma - i \frac{\partial_\mu a}{f_a} \mathbf{c}_q^L \Sigma - i \frac{\partial_\mu a}{f_a} \Sigma \mathbf{c}_q^R, \quad \mathbf{c}_q^L = \mathbf{c}_q^R = \mathbf{c}_q. \quad (2.23)$$

By adding everything together we are therefore able to write

$$D_\mu \Sigma = \partial_\mu \Sigma - ie A_\mu [\mathbf{Q}, \Sigma] - i \frac{\partial_\mu a}{f_a} \{c_q, \Sigma\}, \quad (2.24)$$

which now replaces the spacetime derivative in our ChPT Lagrangian, Eq. (2.10). These results will be very helpful in describing CP -odd dark pions with GeV-scale mass. For instance, in chapter 3 we calculate the width for the decay of a CP -odd dark pion into three SM pions, which competes with $\hat{\pi} \rightarrow \mu^+ \mu^-$ when $m_{\hat{\pi}} \lesssim 1$ GeV. Above a scale $\sim 4\pi f_\pi$ ChPT ceases to be a sensible EFT, since the expansion parameter becomes of order one.

2.2 Electroweak precision tests (EWPT) of the SM

The second tool we are going to need in the analysis of the Z' model, is the treatment of precision tests of the electroweak sector of the SM, which have been extensively performed both at e^+e^- colliders, such as LEP, and hadron colliders, such as the LHC. The observed agreement between the predictions of the SM, which rely on a few input parameters (for instance α , G_F and M_Z) and require the calculation of radiative corrections, and experimental data places important constraints on a variety of models of new physics. Extension of the SM that contain a Z' vector boson are no exception [40].

An important question to address, is how the impact of new physics on EWPT is parametrized. For the type of Z' considered in this thesis, which as we are going to see couples to SM fermions only by mass or kinetic mixing with SM gauge bosons, a simplified description suffices where all new physics effects are absorbed in “oblique” corrections (as they are traditionally known) to the self-energies of the SM vectors [41]. The class of SM extension for which this is possible is known as “universal new physics”.

The most general 1-loop vacuum polarization can be written as:

$$V_\mu \sim \text{[diagram: a circle with diagonal lines]} V'_\nu = i (\Pi_{VV'}(p^2) \eta_{\mu\nu} - \Delta_{VV'}(p^2) p_\mu p_\nu), \quad (2.25)$$

where p denotes the external momentum. The vacuum polarizations are coupled to SM fermionic currents, hence in the limit where the fermion masses are negligible compared to the energy range we are probing, we find that the terms proportional to $\Delta_{VV'}$ are negligible because

$$p^\mu J_\mu^{\text{light}} = \bar{f} p^\mu \gamma_\mu f = m_f \bar{f} f. \quad (2.26)$$

Four types of vacuum polarization exist, namely $VV' = \{W^+W^-, W^3W^3, W^3B, BB\}$. Assuming the new physics to be heavier than the electroweak scale, we can expand as follows

$$\Pi_{VV'}(p^2) \simeq \Pi_{VV'}(0) + p^2 \underbrace{\frac{d\Pi_{VV'}}{dp^2} \Big|_{p^2=0}}_{\Pi'_{VV'}(0)} + \frac{1}{2} p^4 \underbrace{\frac{d^2\Pi_{VV'}}{d(p^2)^2} \Big|_{p^2=0}}_{\Pi''_{VV'}(0)} + \dots \quad (2.27)$$

Therefore we have a grand total of twelve expansion parameters, however, the masslessness of the photon guarantees that $\Pi_{\gamma\gamma}(0) = \Pi_{\gamma Z}(0) = 0$. In addition, we can trade three more parameters for (g, g', v) , where $v \approx 246.2$ GeV in this thesis. Out of initial twelve parameters, we are thus left with just seven [42],

$$\begin{aligned} \hat{S} &= \frac{g}{g'} \Pi'_{3B}(0), & \hat{T} &= \frac{\Pi_{33}(0) - \Pi_{W^+W^-}(0)}{M_W^2}, & \hat{U} &= \Pi'_{W^+W^-}(0) - \Pi'_{33}(0), \\ V &= \frac{M_W^2}{2} (\Pi''_{33}(0) - \Pi''_{W^+W^-}(0)), & X &= \frac{M_W^2}{2} \Pi''_{3B}(0), & Y &= \frac{M_W^2}{2} \Pi''_{BB}(0), & W &= \frac{M_W^2}{2} \Pi''_{33}(0). \end{aligned} \quad (2.28)$$

It is useful to relate \hat{S} , \hat{T} and \hat{U} to the classic Peskin-Takeuchi oblique parameters [43, 44],

$$\hat{S} = \frac{\alpha S}{4s_W^2}, \quad \hat{T} = \alpha T, \quad \hat{U} = -\frac{\alpha U}{4s_W^2}, \quad (2.29)$$

where s_W is the sine of the weak mixing angle.

It is worth mentioning that we define the oblique parameters to only account for new physics effects. The most general expression of the vacuum polarizations does contain the sum of SM radiative corrections and NP effects,

$$\Pi_{VV'}^{\text{tot}} = \Pi_{VV'}^{\text{SM}} + \Pi_{VV'}. \quad (2.30)$$

In chapter 4 we are going to compute the values of the 7 oblique parameters in the Z' model, by integrating out the new particle at tree level.

The EWPT have provided important successes in the past, for instance with the prediction of the top mass. In particular, the contribution of the third generation SM fermions to the T parameter reads [43, 44]

$$T = \frac{N_c}{16\pi s_W^2 c_W^2 M_Z^2} \left[m_t^2 + m_b^2 - 2 \frac{m_t^2 m_b^2}{m_t^2 - m_b^2} \log \left(\frac{m_t^2}{m_b^2} \right) \right] \stackrel{m_t \gg m_b}{\approx} \frac{N_c}{16\pi s_W^2 c_W^2 M_Z^2} \frac{m_t^2}{3}. \quad (2.31)$$

As we can see, T depends quadratically on m_t and is therefore very sensitive to its value. On the other hand, the effect given by the Higgs is much milder [43, 44],

$$T \approx -\frac{3}{16\pi c_W^2} \log \left(\frac{m_h^2}{m_{h,\text{ref}}^2} \right), \quad (2.32)$$

where $m_{h,\text{ref}}$ is a reference value of the Higgs mass. Now T depends only logarithmically m_h , hence giving a much looser constraint. For this reason, only limited information about the Higgs could be gained from indirect measurements, and its direct discovery and the measurement of its mass have been a crucial milestone in the progress of particle physics.

Chapter 3

Confining dark sectors from Neutral Naturalness

As we saw in chapter 1, a dark copy of QCD that confines at scales not far from the GeV is a generic prediction of NN models. This opens up a variety of phenomenological signatures, which are of central importance to this thesis. We begin by reviewing in section 3.1 the situation in the Fraternal Twin Higgs (FTH) model, where the matter content – which includes at most one light Twin quark, the \hat{b} – does not give rise to pNGBs at the bottom of the hadron spectrum. In this case, the lightest dark hadron is either a Twin bottomonium or Twin glueball state. We then introduce in section 3.2 a different model of dark QCD, originally studied in Ref. [32] and inspired by the SUSY NN construction of Refs. [28, 45], where multiple light dark quarks are present and therefore a set of “dark pions” are expected to dominate the phenomenology. Finally, in section 3.3 we perform an example calculation using ChPT, deriving the widths for the decays of the dark pions $\hat{\pi}$ to three SM pions, for $m_{\hat{\pi}} \lesssim 1$ GeV, to illustrate the underlying techniques.

3.1 Dark hadron phenomenology in the Fraternal Twin Higgs

The FTH contains only two Twin quarks, among which the Twin top has mass $y_t f / \sqrt{2} \gg \hat{\Lambda}_{\text{QCD}}$. Therefore, at most one quark (the \hat{b}) can be light. One-flavor QCD does not give rise to pNGBs; rather, the hadron spectrum is dominated by quarkonia with masses $\sim \hat{\Lambda}_{\text{QCD}}$ if the Twin bottom is light, or glueballs if the Twin bottom is heavy. In both cases precise quantitative results require lattice calculations, which are more available for glueballs [46, 47] than for quarkonia [48]. Here we necessarily limit ourselves to a brief and qualitative overview.

The spectrum of Twin hadrons, and the associated phenomenology, strongly depend on the hierarchy between $m_{\hat{b}}$ (which is largely a free parameter, except for the loose requirement that $\hat{y}_{\hat{b}}$ does not introduce a new hierarchy problem) and $\hat{\Lambda}_{\text{QCD}}$. If the Twin bottom is heavy, the infrared spectrum is dominated by glueballs, namely bound states made of only (Twin) gluons. Lattice calculations for pure- $SU(3)$ glue QCD provide the J^{PC} of the lightest few glueballs and the ratios of their masses to the confinement scale [47]. Importantly, the lightest glueball, usually called $\hat{G}_{0^{++}}$, has mass $m_0 \approx 6.8 \hat{\Lambda}_{\text{QCD}}$ and $J^{PC} = 0^{++}$. The fact that $\hat{G}_{0^{++}}$ shares the quantum numbers of the Higgs leads to interesting phenomenology, as discussed below.

On the other hand, if the Twin bottom mass is small enough, the lightest hadrons are $\bar{\hat{b}}\hat{b}$ “bottomonium” states. In analogy to the SM bottomonia we denote the lightest Twin bottomonium, which has mass $\sim 2(m_{\hat{b}} + \hat{\Lambda}_{\text{QCD}})$, as $\hat{\eta}_{\hat{b}}$ ($J^{PC} = 0^{-+}$). Above it we find a spin-1 state, $\hat{\Upsilon}$, with $J^{PC} = 1^{--}$. Next, we expect a 0^{++} scalar $\hat{\chi}_{\hat{b}0}$, which can mix with the Higgs.

The interaction between the SM and the strongly interacting dark sector is mediated, irreducibly,

by the Higgs. This leads to striking phenomenological signatures that can be probed at particle accelerators. To sketch these features we assume the Twin leptons are heavier than the Twin hadrons; this is a consequential choice, implying that the Twin hadrons decay directly to SM particles.

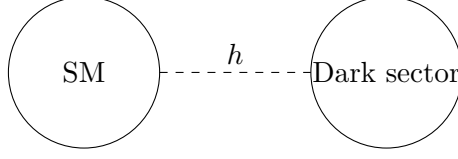


Figure 3.1: Diagrammatic depiction of the portal between the SM and dark sector in the FTH model.

The first type of communication is through an effective interaction of the Higgs with the Twin gluons, dominantly mediated by a Twin top loop.

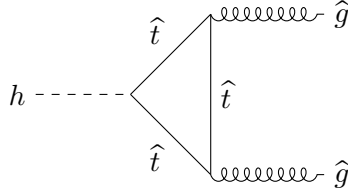


Figure 3.2: Twin top-induced effective interaction between the physical Higgs and the dark gluons.

Since $m_h \ll 2m_{\hat{t}}$, we obtain (see for example Ref. [26])

$$\mathcal{L}_{\text{eff}} \supset -\frac{\hat{\alpha}_s}{12\pi} \frac{v}{f^2} h \hat{G}_{\mu\nu}^a \hat{G}^{a,\mu\nu}, \quad (3.1)$$

which is responsible both for the $h \rightarrow \hat{g}\hat{g}$ process, allowing colliders such as the LHC to access the dark sector, and for the decay of \hat{G}_{0++} , with

$$c\tau_{\hat{G}_{0++}} \approx 1 \text{ cm} \left(\frac{5 \text{ GeV}}{\hat{\Lambda}_{\text{QCD}}} \right)^7 \left(\frac{f}{1 \text{ TeV}} \right)^4, \quad (3.2)$$

valid for $2m_\tau < m_0 < M_W$. This is an important result, showing that the lightest Twin glueball has a *macroscopic* decay length. Thus, a typical FTH event consists [49] in a rare decay of the Higgs to Twin gluons, followed by parton showering and hadronization in the dark sector. The outgoing particles are a few Twin glueballs. Among them, one \hat{G}_{0++} can travel a macroscopic distance before decaying to SM particles, giving rise to a displaced signature. Similar considerations apply to the second type of portal between the SM and Twin sectors, namely the coupling of h to the Twin bottom

$$\mathcal{L}_{\text{eff}} \supset -\frac{\hat{y}_b}{\sqrt{2}} \frac{v}{f} h \hat{b}\hat{b}. \quad (3.3)$$

This interaction mediates Higgs decays to \hat{b} pairs, and is also responsible for setting the lifetime of the $\hat{\chi}_{b0}$ bottomonium. Rather than delve more deeply into the phenomenology of the FTH, we choose to make a further step and, in the next section, we discuss a dark QCD sector where more than one light quark flavor is present. As we are going to show, this leads to a qualitatively different picture due to the existence of light pNGB modes.

3.2 Toward a theory of dark pions

The FTH specifically, and the Twin Higgs more generally, are a popular incarnation of NN, but by no means the only one, as reviewed for example in Ref. [50]. Here we consider another class of confining dark sector models, characterized by two essential features:

- More than one light dark quark flavors are present, so that pNGBs appear at the bottom of the hadron spectrum;
- The interaction between the SM and the dark sector is mediated by the Z boson (in addition to the Higgs boson).

The original motivation for this class of models is a SUSY NN construction, called “tripled top”, that was built in Refs. [28, 45]. We do not take a top-down approach, however, but prefer to tackle the problem in a bottom-up perspective. In fact, two classes of UV completions can be envisaged for an interaction of the form $Z\bar{\psi}\psi$ between the Z boson and the dark quarks. In the first class, which was extensively discussed in Ref. [32], the completion contains some heavy dark quarks Q , doublets under the SM weak interactions, which allow for Yukawa interactions coupling the Q , the light dark quarks ψ , and the SM Higgs doublet H ; this is depicted in the left diagram in Fig. 3.3.¹

The second class of models, which has not been discussed before and is the subject of chapters 4 and 5 of this thesis, is shown by the right diagram in Fig. 3.3. Here the Z portal is obtained by mixing (through mass and/or kinetic terms) the Z boson with a Z' vector, the latter being coupled to the dark quarks at tree level.

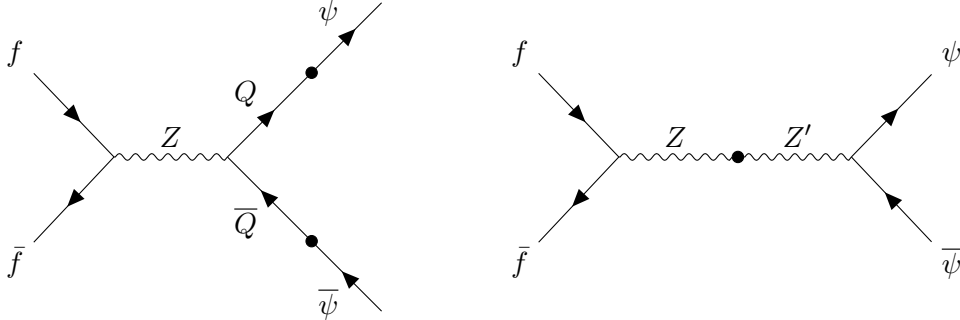


Figure 3.3: Different UV completions of a Z portal to the dark sector. On the left side we show the model studied in Ref. [32] and reviewed in this chapter. On the right side we display the Z' model discussed for the first time in chapters 4 and 5.

Let us now review the model containing the heavy fermions Q [32]. The UV Lagrangian reads

$$-\mathcal{L} = \bar{Q}_L \mathbf{Y} \psi_R H + \bar{Q}_R \tilde{\mathbf{Y}} \psi_L H + \bar{Q}_L \mathbf{M} Q_R + \bar{\psi}_L \boldsymbol{\omega} \psi_R + \text{h.c.}, \quad (3.4)$$

where \mathbf{Y} , $\tilde{\mathbf{Y}}$, \mathbf{M} and $\boldsymbol{\omega}$ are $N \times N$ matrices in the flavor space. Following the inspiration from NN, the masses \mathbf{M} of the heavy fermions are expected to be at the TeV scale, since their supersymmetric partners would play the role of scalar top partners. On the other hand, the masses of the light dark quarks are smaller than $\hat{\Lambda}_{\text{QCD}}$. We assume $N \geq 2$, leading to the expectation of chiral symmetry breaking and $N^2 - 1$ pNGBs, which we call “dark pions” and denote with $\hat{\pi}$.

Before we elucidate the details of the model, we sketch the associated phenomenology: owing to the large Z production rate at the LHC, $Z \rightarrow \bar{\psi}\psi$ decays are expected to be the most important mechanism

¹Incidentally, we note that heavy vector-like fermions with the quantum numbers of Q , namely SM electroweak and dark color charges, also appear in non-SUSY UV completions of the Twin Higgs; in the original model of Ref. [17] these fermions render finite the Higgs potential, cutting off the residual logarithmic divergences. Their phenomenology has also been studied in that context [51].

of dark sector production. Following dark parton shower and hadronization a number of dark pions is obtained, which can decay back to the SM with macroscopic lifetimes. As we will describe, some of the dark pions behave as composite axion-like particles (ALPs), whereas others behave as composite Higgs-mixed scalars.

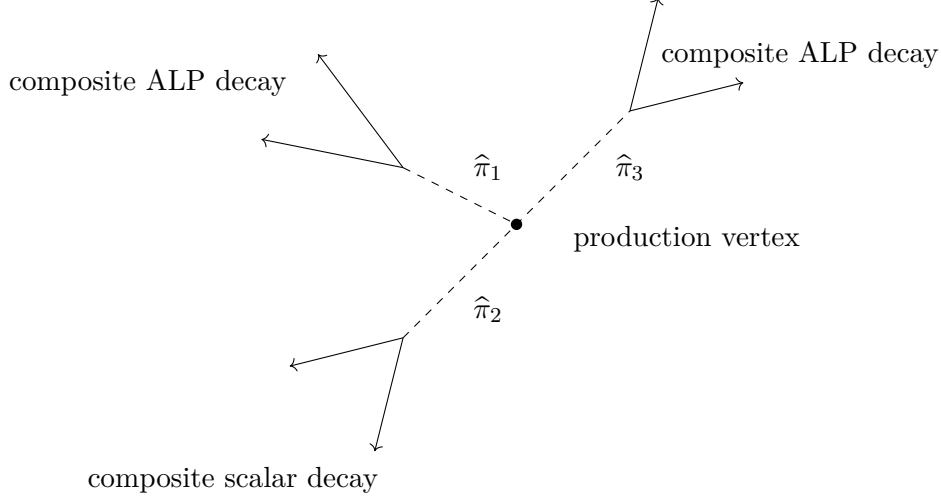


Figure 3.4: A sketch of dark pion phenomenology, assuming $N = 2$. All dark pions typically have macroscopic lifetimes. The $\hat{\pi}_{1,3}$ behave as composite ALPs and the $\hat{\pi}_2$ as a composite scalar mixed with the Higgs.

From now on we assume $N = 2$ light flavors. As a first step, we integrate out the heavy Q to obtain an effective Lagrangian where the SM is coupled to the light dark quarks. We find

$$\begin{aligned} \mathcal{L}_{\text{EFT}} = & \frac{1}{2} \bar{\psi}_R \mathbf{Y}^\dagger \mathbf{M}^{-2} \mathbf{Y} [|H|^2 i \not{D} + i \gamma^\mu H^\dagger D_\mu H] \psi_R + \text{h.c.} \\ & + \frac{1}{2} \bar{\psi}_L \tilde{\mathbf{Y}}^\dagger \mathbf{M}^{-2} \tilde{\mathbf{Y}} [|H|^2 i \not{D} + i \gamma^\mu H^\dagger D_\mu H] \psi_L + \text{h.c.} \\ & - \bar{\psi}_L \boldsymbol{\omega} \psi_R + \bar{\psi}_L \tilde{\mathbf{Y}}^\dagger \mathbf{M}^{-1} \mathbf{Y} \psi_R |H|^2 + \text{h.c.} \end{aligned} \quad (3.5)$$

We now show that this effective Lagrangian is responsible for the decay of dark pions to SM particles. It is important to note that in our scenario $\hat{\pi}_{1,3}$ have $J^{PC} = 0^{-+}$, whereas $\hat{\pi}_2$ has 0^{--} . The CP -odd dark pions decay to SM particles via Z boson exchange, whereas the decay of CP -even dark pions is mediated by the Higgs portal. From Eq. (3.5) we can write down the interaction between the dark quarks and the Z ,

$$-\frac{g_Z v^2}{4} \left[\bar{\psi}_R \mathbf{Y}^\dagger \mathbf{M}^{-2} \mathbf{Y} \gamma^\mu \psi_R + \bar{\psi}_L \tilde{\mathbf{Y}}^\dagger \mathbf{M}^{-2} \tilde{\mathbf{Y}} \gamma^\mu \psi_L \right] Z_\mu \quad (3.6)$$

where $g_Z \equiv \sqrt{g^2 + g'^2}$. The mass matrix of light dark quarks receives two contributions, i.e. $\boldsymbol{\omega} - \tilde{\mathbf{Y}}^\dagger \mathbf{M}^{-1} \mathbf{Y} v^2/2$, and is diagonalized through unitary transformations $\psi_{L,R} = U_{L,R} \psi'_{L,R}$. After these transforms, Eq. (3.6) can be rewritten as

$$-\frac{g_Z}{2} \left(\bar{\psi}'_R \mathbf{A} \gamma^\mu \psi'_R + \bar{\psi}'_L \tilde{\mathbf{A}} \gamma^\mu \psi'_L \right) Z_\mu = -\frac{g_Z}{4} \sum_{q=0}^3 \left\{ \text{Tr}[\sigma_q (\mathbf{A} + \tilde{\mathbf{A}})] j_q^\mu + \text{Tr}[\sigma_q (\mathbf{A} - \tilde{\mathbf{A}})] j_{5q}^\mu \right\} Z_\mu, \quad (3.7)$$

where $\sigma_0 \equiv \mathbb{I}$ and

$$\mathbf{A} \equiv \frac{v^2}{2} U_R^\dagger \mathbf{Y}^\dagger \mathbf{M}^{-2} \mathbf{Y} U_R, \quad \tilde{\mathbf{A}} \equiv \frac{v^2}{2} U_L^\dagger \tilde{\mathbf{Y}}^\dagger \mathbf{M}^{-2} \tilde{\mathbf{Y}} U_L, \quad (3.8)$$

and

$$j_q^\mu = j_{Rq}^\mu + j_{Lq}^\mu, \quad j_{5q}^\mu = j_{Rq}^\mu - j_{Lq}^\mu, \quad j_{L,Rq}^\mu = \bar{\psi}'_{L,R} \gamma^\mu \frac{\sigma_q}{2} \psi'_{L,R}. \quad (3.9)$$

We are now able to rewrite everything in the hadronic basis. In analogy to the SM, we define the dark pion decay constant $f_{\hat{\pi}}$ from

$$\langle 0 | j_{5b}^\mu(0) | \hat{\pi}_c(p) \rangle = -i \delta_{bc} f_{\hat{\pi}} p^\mu, \quad (3.10)$$

where the same normalization used for the SM in Eq. (2.7) has been adopted.

It is possible to integrate out the Z in the static limit to obtain an effective interaction Lagrangian between the dark pions and the SM fermions f . Only the axial part of the Z current survives, because $(\partial_\mu \hat{\pi}_b) \bar{f} \gamma^\mu f \simeq -\hat{\pi}_b \partial_\mu (\bar{f} \gamma^\mu f) = 0$, so we get

$$-\frac{g_Z^2 f_{\hat{\pi}}}{8M_Z^2} \text{Tr}[\sigma_b(\mathbf{A} - \tilde{\mathbf{A}})] (\partial_\mu \hat{\pi}_b) \bar{f} \gamma^\mu T_{Lf}^3 \gamma_5 f, \quad (3.11)$$

with T_{Lf}^3 is eigenvalue of the third generator of $SU(2)_L$. This can be framed as an ALP Lagrangian

$$-\frac{\partial_\mu a}{f_a} c_f \bar{f} \gamma^\mu \gamma_5 f, \quad \frac{1}{f_a^{(b)}} \equiv \frac{g_Z^2 f_{\hat{\pi}}}{8M_Z^2} \text{Tr}[\sigma_b(\mathbf{A} - \tilde{\mathbf{A}})], \quad c_f = T_{Lf}^3, \quad (3.12)$$

where $f_a^{(b)}$ is called the *effective decay constant* of the (composite) ALP $\hat{\pi}_b = a$. From this one readily computes the decay rate into SM fermions,

$$\Gamma(a \rightarrow \bar{f} f) = N_c^f \frac{c_f^2 m_f^2}{2\pi f_a^2} m_a \left(1 - 4 \frac{m_f^2}{m_a^2}\right)^{1/2}, \quad (3.13)$$

where N_c^f is a color factor. Assuming CP conservation, $\hat{\pi}_{1,3}$ can decay though the Z portal to SM states, whereas $\hat{\pi}_2$ does not because

$$\text{Tr}[\sigma_2(\mathbf{A} - \tilde{\mathbf{A}})] = i[(\mathbf{A} - \tilde{\mathbf{A}})_{12} - (\mathbf{A} - \tilde{\mathbf{A}})_{12}^*] = 0, \quad (3.14)$$

where the hermiticity of \mathbf{A} and $\tilde{\mathbf{A}}$ has been used.

For dark pions with GeV scale masses, an important complication arises from the need to describe exclusive decays to SM hadrons, rather than perturbative decays to SM quarks. An exhaustive analysis has been performed in Ref. [32], whose results are summarized in Fig. 3.5, where decay widths and branching ratios are shown for arbitrary $m_a < 3$ GeV and $c_f = T_{Lf}^3$. We see that the decay to $\mu^+ \mu^-$, calculated according to Eq. (3.13), dominates in the region $2m_\mu < m_a \lesssim m_{\eta'}$. However, hadronic decays are already important for $m_a \lesssim m_{\eta'}$ and become completely dominant for $m_a \gtrsim 1$ GeV. For energy scales up to the mass of the η' , the calculations are performed using the effective theory of pNGBs in QCD, namely Chiral Perturbation Theory (ChPT). In section 3.3 we are going to perform an example calculation of this type, using ChPT. For even larger ALP masses one must resort to a phenomenological description based on resonance exchange, which will not be treated here in any detail. Let us now focus on the total decay width shown in Fig. 3.5, and convert it to meters in order to gain some intuition on the phenomenology. Choosing $m_{\hat{\pi}} = 800$ MeV as example, we find

$$c\tau_{\hat{\pi}} = 0.40 \text{ m} \left(\frac{f_a}{\text{PeV}}\right)^2, \quad (3.15)$$

implying that the CP -odd dark pions behave as long-lived particles in accelerator experiments [52].

Similarly to what has been shown until now for $\hat{\pi}_{1,3}$, it can be proven that the $\hat{\pi}_2$ decays to SM particles though the Higgs portal. Starting from the last line of Eq. (3.5) we can extract the interaction between the dark light quarks and a single Higgs,

$$\bar{\psi}'_L \mathbf{B} \psi'_R h + \text{h.c.} = \frac{1}{2} \bar{\psi}' \left[(\mathbf{B} + \mathbf{B}^\dagger) + (\mathbf{B} - \mathbf{B}^\dagger) \gamma_5 \right] \psi' h, \quad \mathbf{B} \equiv v U_L^\dagger \tilde{\mathbf{Y}}^\dagger \mathbf{M}^{-1} \mathbf{Y} U_R. \quad (3.16)$$

The dark quarks have already been rotated to the mass basis. Only the piece containing γ_5 between square parentheses survives and can be written as

$$-\frac{1}{2} \sum_{q=0}^3 \text{Tr}[i\sigma_q(\mathbf{B} - \mathbf{B}^\dagger)] \bar{\psi}' \frac{i\sigma_q}{2} \gamma_5 \psi' h. \quad (3.17)$$

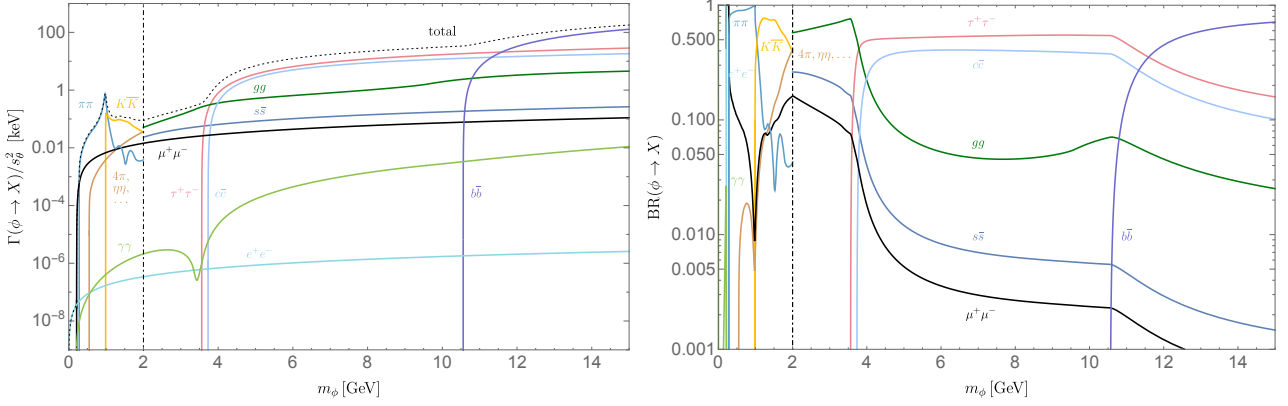


Figure 3.6: Decay widths (left panel) and branching ratios (right panel) for a light CP -even scalar interacting with the SM through Higgs mixing. The dot-dashed line at $m_\phi = 2$ GeV indicates the mass where the description of hadronic decays switches from dispersive methods to a perturbative spectator model, following Ref. [53]. This figure is taken from Ref. [32].

3.2.1 Constraints from Z and h invisible decays

Equations (3.6) and (3.16) imply that both the Z and Higgs bosons can decay to dark hadron final states. If we suppose that the dark hadrons are sufficiently long lived to be, in first approximation, invisible to experiments, we can derive some significant constraints on the parameter space of the model, by employing existing measurements of the invisible Z and h decay widths.

From (3.6) we can immediately evaluate the decay width of the Z into dark quarks, for which we find

$$\Gamma(Z \rightarrow \bar{\psi}'\psi') = \frac{N_d M_Z^3}{96\pi\sqrt{2}G_F} \left\{ \text{Tr} \left[(\mathbf{Y}^\dagger \mathbf{M}^{-2} \mathbf{Y})^2 + (\mathbf{Y} \rightarrow \tilde{\mathbf{Y}}) \right] \right\}, \quad (3.21)$$

where N_d is the number of dark colors. Taking for example $\mathbf{M} = M\mathbb{I}$ and imposing that $\Gamma_{\text{inv}}^Z < 2$ MeV at 95% CL [54], we obtain

$$M \gtrsim 0.7 \text{ TeV} \left(\frac{N_d \text{Tr}(\mathbf{Y}\mathbf{Y}^\dagger \mathbf{Y}\mathbf{Y}^\dagger) + (\mathbf{Y} \rightarrow \tilde{\mathbf{Y}})}{3} \right)^{1/4}. \quad (3.22)$$

A similar calculation can be done for the invisible decays of the Higgs starting from Eq. (3.16). In this case we have

$$\Gamma(h \rightarrow \bar{\psi}'\psi') = \frac{N_d m_h}{8\pi\sqrt{2}G_F} \text{Tr} \left[\mathbf{Y}^\dagger \mathbf{M}^{-1} \tilde{\mathbf{Y}} (\mathbf{Y}^\dagger \mathbf{M}^{-1} \tilde{\mathbf{Y}})^\dagger \right]. \quad (3.23)$$

Assuming again $\mathbf{M} = M\mathbb{I}$ and requiring that $\text{BR}(h \rightarrow \text{inv}) < 0.13$ at 95% CL [55] we arrive at

$$M \gtrsim 0.4 \text{ TeV} \left(\frac{N_d \text{Tr}(\mathbf{Y}\mathbf{Y}^\dagger \tilde{\mathbf{Y}}\tilde{\mathbf{Y}}^\dagger)}{3 \cdot 10^{-4}} \right)^{1/2}, \quad (3.24)$$

where $Y \sim \tilde{Y} \sim 0.1$ has been taken as reference value for the Yukawas. Notice that for $Y \sim \tilde{Y} \sim 1$ one finds a very strong bound from Higgs decays, $M \gtrsim 40$ TeV. However, this constraint can be easily loosened by taking a hierarchy between the Yukawas, for instance $Y \gg \tilde{Y}$, in which case the leading bound stems from Z decays and the parameter region with $Y \sim 1$, $M \sim \text{TeV}$ is still allowed [32].

3.3 Hadronic decays of dark pions: an example ChPT calculation

To illustrate the ChPT techniques involved in the study of GeV-scale dark sector particles, here we calculate the decay widths for the decays of an ALP into three SM pions, $a \rightarrow 3\pi$. Our starting point

is the leading ChPT Lagrangian, Eq. (2.10), augmented by the covariant derivative in Eq. (2.24),

$$\text{Tr}[(D_\mu \Sigma)^\dagger (D^\mu \Sigma)] \supset -\frac{\partial_\mu a}{f_a} \frac{8}{f_\pi} \text{Tr}[\mathbf{c}_q \partial^\mu \mathbf{P}], \quad (3.25)$$

where $\mathbf{c}_q = \text{diag}(c_u, c_d, c_s)$. Thus, at leading order in \mathbf{P}/f_π we obtain a kinetic mixing between the ALP and the SM pseudoscalar mesons. In fact, we can write

$$\mathcal{L}_{\text{kin}} \supset -\frac{f_\pi}{f_a} \partial_\mu a \sum_{P=\pi_0, \eta, \eta'} K_{aP} \partial^\mu P \quad (3.26)$$

with

$$K_{a\pi_0} = c_u - c_d, \quad K_{a\eta} = \sqrt{\frac{2}{3}}(c_u + c_d - c_s), \quad K_{a\eta'} = \frac{1}{\sqrt{3}}(c_u + c_d + 2c_s). \quad (3.27)$$

The kinetic mixing is diagonalized at order $f_\pi/f_a \ll 1$ by means of the following field redefinitions [56],

$$a \rightarrow a - \frac{f_\pi}{f_a} \sum_{P=\pi_0, \eta, \eta'} \frac{m_P^2}{m_a^2} \langle \mathbf{aP} \rangle P, \quad P \rightarrow P + \frac{f_\pi}{f_a} \langle \mathbf{aP} \rangle a, \quad \langle \mathbf{aP} \rangle = \frac{m_a^2 K_{aP}}{m_a^2 - m_P^2}, \quad (3.28)$$

where we have defined $\langle \dots \rangle \equiv 2 \text{Tr}(\dots)$. Recall that in this thesis we neglect the isospin breaking parameter $\delta_I = (m_d - m_u)/(m_d + m_u)$, which greatly reduces the complexity of our calculations. In fact, we can assign to the ALP a $U(3)$ representation [56]

$$\mathbf{a} = \langle \mathbf{a}\pi_0 \rangle \pi_0 + \langle \mathbf{a}\eta \rangle \eta + \langle \mathbf{a}\eta' \rangle \eta' \quad (3.29)$$

with

$$\pi_0 = \frac{1}{2} \text{diag}(1, -1, 0), \quad \eta = \frac{1}{\sqrt{6}} \text{diag}(1, 1, -1), \quad \eta' = \frac{1}{2\sqrt{3}} \text{diag}(1, 1, 2). \quad (3.30)$$

In this way we can write Σ as

$$\Sigma = \exp \left[2i \left(\frac{\mathbf{P}}{f_\pi} + \mathbf{a} \frac{a}{f_a} \right) \right] \equiv \exp \left(2i \frac{\tilde{\mathbf{P}}}{f_\pi} \right). \quad (3.31)$$

We now want to find an explicit expression for the $a\pi^3$ interactions. Expanding the kinetic term of the ChPT Lagrangian up to $\mathcal{O}(\tilde{\mathbf{P}}^3/f_\pi^3)$, we find

$$\mathcal{L}_{\text{kin}} \supset \frac{\langle \mathbf{a}\pi_0 \rangle}{3f_\pi f_a} (\pi^+ \pi_0 \partial_\mu a \partial^\mu \pi^- - a \pi_0 \partial_\mu \pi^+ \partial^\mu \pi^- - \pi^+ \pi^- \partial_\mu a \partial^\mu \pi_0 + a \pi^+ \partial_\mu \pi^- \partial^\mu \pi_0 + \text{h.c.}). \quad (3.32)$$

Importantly, only terms involving $a\pi^+ \pi^+ \pi_0$ appear, but no $a(\pi_0)^3$ pieces. A similar calculation is done for the mass term in the Lagrangian, where one needs to expand up to $\mathcal{O}(\tilde{\mathbf{P}}^4/f_\pi^4)$,

$$\mathcal{L}_{\text{mass}} \supset \frac{B_0 m \langle \mathbf{a}\pi_0 \rangle}{3f_a f_\pi} [a(\pi_0)^3 + 2a\pi^+ \pi^- \pi_0]. \quad (3.33)$$

We are ready to evaluate the ALP decay widths. The amplitude for $a \rightarrow 3\pi_0$ is read off $\mathcal{L}_{\text{mass}}$,

$$i\mathcal{M}(a \rightarrow 3\pi_0) = i \frac{m_\pi^2}{f_\pi f_a} \langle \mathbf{a}\pi_0 \rangle \Theta(m_{\eta'} - m_a), \quad (3.34)$$

where the Heaviside theta function simply indicates that our ChPT description cannot be trusted above $m_a \sim m_{\eta'}$. As for $a \rightarrow \pi^+ \pi^- \pi_0$, from Eq. (3.32) we derive the Feynman rule



$$(3.35)$$

$$= i \frac{\langle \mathbf{a}\pi_0 \rangle}{3f_\pi f_a} [-p_a \cdot p_- - p_a \cdot p_+ + 2p_- \cdot p_+ + 2p_a \cdot p_0 - p_- \cdot p_0 - p_+ \cdot p_0] \Theta(m_{\eta'} - m_a).$$

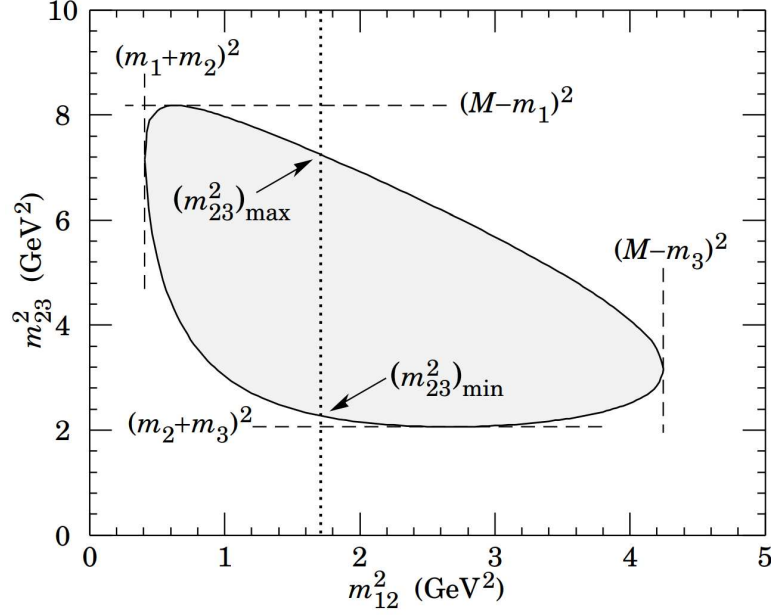


Figure 3.7: Dalitz plot of a three-body decay, showing the allowed regions of m_{12}^2 and m_{23}^2 . Figure taken from Ref. [36].

Applying four-momentum conservation and including the contribution from Eq. (3.33), we obtain

$$i\mathcal{M}(a \rightarrow \pi^+ \pi^- \pi_0) = i \frac{\langle \mathbf{a} \pi_0 \rangle}{3f_\pi f_a} \left[3m_{12}^2 - m_a^2 - 2m_\pi^2 \right] \Theta(m_{\eta'} - m_a), \quad (3.36)$$

where we have defined $m_{12}^2 = (p_+ + p_-)^2$. The decay widths are given by

$$\Gamma(a \rightarrow 3\pi) = \frac{k}{2Sm_a} \int |\mathcal{M}(a \rightarrow 3\pi)|^2 d\Phi_3, \quad (3.37)$$

where S denotes a multiplicity factor for identical daughter particles ($S = 1$ for $a \rightarrow \pi^+ \pi^- \pi_0$ and $S = 3!$ for $a \rightarrow 3\pi_0$). The constant $k = 2.7$, which approximately accounts for the important higher-order corrections, is estimated from $\eta^{(\prime)} \rightarrow 3\pi$ data [56]. The differential decay width can be written as [36]

$$d\Gamma = \frac{k|\overline{\mathcal{M}}|^2}{S(2\pi)^3 32M^3} dm_{12}^2 dm_{23}^2, \quad (3.38)$$

where $m_{ij}^2 = (p_i + p_j)^2$ and M denotes the mass of the decaying particle. The extrema of integration are fixed by kinematic constraints and are illustrated in Fig. 3.7. One has

$$\Gamma = \int_{(m_1+m_2)^2}^{(M-m_3)^2} dm_{12}^2 \int_{(m_{23}^2)_{\min}}^{(m_{23}^2)_{\max}} dm_{23}^2 \frac{k|\overline{\mathcal{M}}|^2}{S(2\pi)^3 32M^3} \quad (3.39)$$

with

$$(m_{23}^2)_{\min, \max} = \frac{(M^2 - m_1^2 + m_2^2 - m_3^2)^2}{4m_{12}^2} - \left(\sqrt{\frac{(-m_1^2 + m_2^2 + m_{12}^2)^2}{4m_{12}^2} - m_2^2} \pm \sqrt{\frac{(-M^2 + m_3^2 + m_{12}^2)^2}{4m_{12}^2} - m_3^2} \right). \quad (3.40)$$

The decay widths are shown in Fig. 3.8 as functions of m_a , setting $c_f = T_{L_f}^3$ so that $c_u = -c_d = -c_s = 1/2 \rightarrow K_{a\pi_0} = 1$. Furthermore, we have set $m_1 = m_2 = m_3 = m_\pi = 140$ MeV. For reference, the decay width into muons has also been depicted. A few comments are in order concerning the

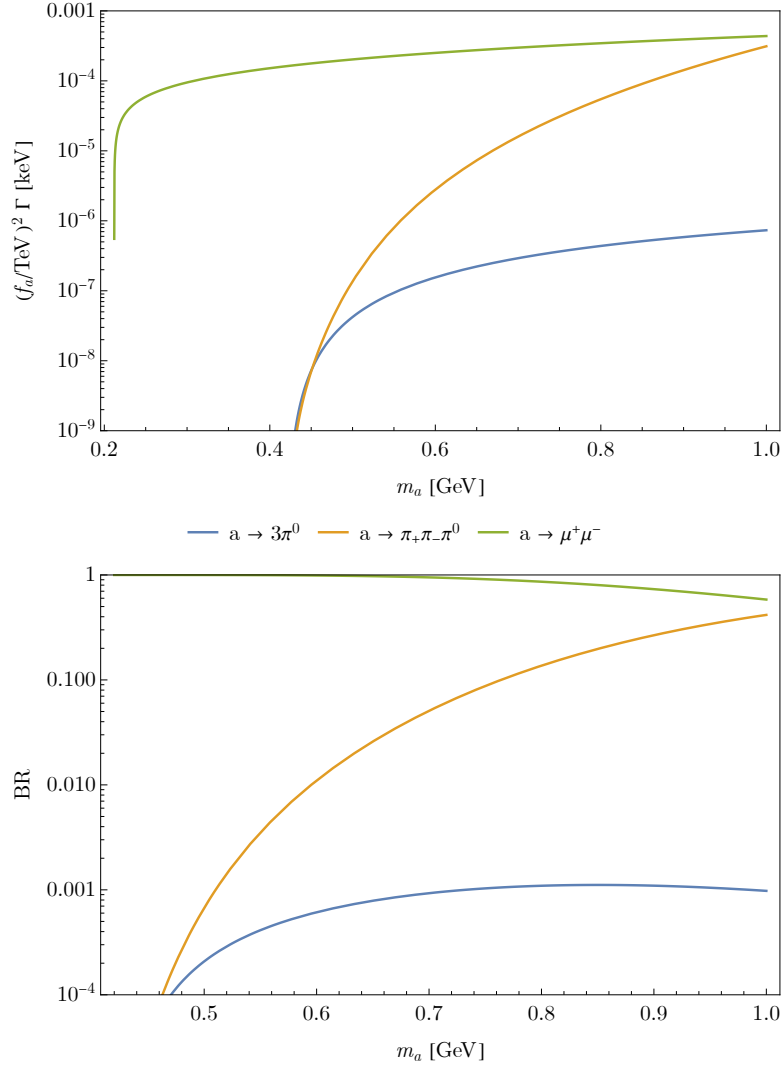


Figure 3.8: Widths (top) and branching ratios (bottom) for different decay channels open to CP -odd dark pions, which behave as composite ALPs a . For the computation of the branching ratios we have considered as total decay width only the sum of the depicted decay modes, neglecting sub-leading contributions coming, for example, from the ALP decay into e^+e^- or $\gamma\gamma$.

comparison of our simplified results with the full calculation displayed in Fig. 3.5. First, we see differences at $m_a = m_{\eta^{(\prime)}}$, which are due to our choice of neglecting isospin breaking originating from $m_u \neq m_d$. In fact, in the full calculation one finds that Eqs. (3.34) and (3.36) both acquire terms proportional to $\delta_I \langle \mathbf{a} \eta^{(\prime)} \rangle$. Second, taking for example $m_a = 800$ MeV we observe that the ALP decay width into $3\pi^0$ is two orders of magnitude smaller than the one into $\pi^+\pi^-\pi_0$, whereas in Fig. 3.5 the two differ only by one order of magnitude. The reason for this discrepancy lies again in the fact that here we have neglected the isospin breaking controlled by δ_I . Third, we recall that for $m_a \gtrsim m_{\eta'}$ the ChPT expansion ceases to be meaningful and one must resort to other methods, such as phenomenological models based on resonance exchange (typically implemented by assuming vector meson dominance) [32].

This concludes our short review of the model with heavy Q fermions. We are now ready to introduce and analyze the Z' model, which will be the subject of chapters 4 and 5.

Chapter 4

Z' model and constraints

We are now ready to study the model of interest for this thesis, namely the UV completion of the Z portal to the dark sector that contains a new Z' vector. The goal of the present chapter and the next, is to investigate this model for the first time and compare it with the UV completion involving heavy fermions, which was presented in section 3.2. Our discussion here will partly follow the classic work [40], though the results of the calculations are new.¹ In the Z' model the dark fermions are charged under a spontaneously broken $U(1)'$, whereas the SM fermions are assumed to be neutral under this new symmetry. The mass of the Z' originates from the vacuum expectation value of a new scalar Φ , charged under $U(1)'$. As a result, the communication between SM and dark sector proceeds in two ways: 1) through mixing of the Z' with the SM electroweak gauge bosons, either of mass or kinetic type; and 2) through mixing between the SM Higgs h and the radial mode of Φ :

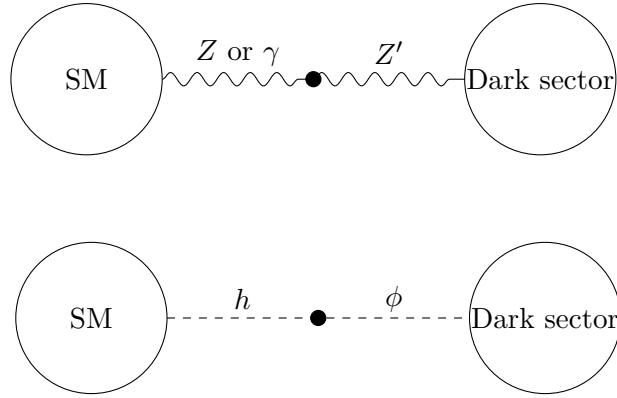


Figure 4.1: Depiction of the possible portals between the SM and the dark sector in the Z' model.

The BSM Lagrangian of the model can be written as

$$\mathcal{L} \supset \mathcal{L}_{Z'} + \mathcal{L}_{\text{mixing}} + \mathcal{L}_{\Phi} + \mathcal{L}_{\text{dark mass}} , \quad (4.1)$$

where

$$\mathcal{L}_{Z'} = -\frac{1}{4}\hat{Z}'_{\mu\nu}\hat{Z}'^{\mu\nu} + \frac{1}{2}\widehat{M}_{Z'}^2\hat{Z}'_{\mu}\hat{Z}'^{\mu} - g_D \sum_i [\bar{\psi}_{Li} X_{Li} \gamma^{\mu} \psi_{Li} + \bar{\psi}_{Ri} X_{Ri} \gamma^{\mu} \psi_{Ri}] \hat{Z}'_{\mu} , \quad (4.2)$$

$$\mathcal{L}_{\text{mixing}} = \delta\widehat{M}^2\hat{Z}_{\mu}\hat{Z}'^{\mu} - \frac{\sin\chi}{2}\hat{Z}'_{\mu\nu}\hat{B}^{\mu\nu} , \quad (4.3)$$

¹Because we adopt the notation of Ref. [40], here and in chapter 5 we use the $D_{\mu} = \partial_{\mu} + igA_{\mu}$ sign convention for the covariant derivative, differently from the first three chapters. We apologize for this switch in notation.

$$\mathcal{L}_\Phi = -\zeta_{ij}\bar{\psi}_{Li}\psi_{Rj}\Phi + \text{h.c.} - \kappa\Phi^*\Phi H^\dagger H, \quad (4.4)$$

and

$$\mathcal{L}_{\text{dark mass}} = -m_{ij}\bar{\psi}_{Li}\psi_{Rj} + \text{h.c.} \quad (4.5)$$

The hats over gauge fields denote that these are not yet the physical states, which we are going to find momentarily by means of field transformations. Several comments are in order. First, we have not written explicitly some terms, such as for example the $SU(N_d)$ -covariant kinetic terms of the dark fermions. Second, we have written the \hat{Z}' mass explicitly; we have in mind that it dominantly arises from the vev of Φ , though we implicitly assume also the existence of a second scalar doublet H' , charged under $U(1)'$, which is responsible for the mass mixing term $\delta\widehat{M}^2$ in Eq. (4.3). In general, one should perform a more complete analysis that also includes the physical scalar degrees of freedom belonging to H' , but this goes beyond our scope here, so we simply assume those modes to be heavy and decoupled. Third, beside mass mixing we have included a kinetic mixing term, parametrized by $\sin\chi$ since its coefficient needs to be smaller than 1 in absolute value to ensure positivity of the kinetic energy. In the next chapter we are going to show that mass and kinetic mixings play very different role in the dark sector phenomenology: $\sin\chi$ cannot mediate the decay of dark pions, whereas $\delta\widehat{M}^2$ does. Fourth, in the dark fermion Lagrangian the matrices m_{ij} and ζ_{ij} have structures that depend on the specific realization, in particular on the $U(1)'$ charge assignments. Several entries are typically vanishing in a given model. Once the angular mode of Φ is eaten to give mass to the Z' , one is left with a physical scalar ϕ that mixes with h through the κ quartic coupling in Eq. (4.4). This will also play a role in dark hadron phenomenology, contributing to the decay of the CP -even dark pions.

4.1 Constraints from EWPT

As a first step in the analysis of our model, we calculate the constraints on the Z' model from EWPT. Since our Z' does not couple to SM fermions at tree level, we are dealing with a “universal” type of new physics, which simplifies the discussion. It should be mentioned that Z' vectors are, in general, not universal.

We have already showed in section 2.2 that, when dealing with heavy new physics, we can parametrize the deviations from the SM by means of 7 form factors built out of the vacuum polarizations $\Pi_{VV'}(p^2)$ of the SM gauge bosons. Taking as an example the B propagator, we have in the Z' model

$$B_\mu \sim \text{blob} \sim B_\nu = B_\mu \sim B_\nu + B_\mu \sim \text{blob} \sim \hat{Z}' \sim \text{blob} \sim B_\nu + \dots, \quad (4.6)$$

where the dots represent subleading corrections. The Z' contributes at tree level, so in order to evaluate the EWPT parameters we can either proceed diagrammatically, or by integrating out the Z' via the equations of motion. Here we choose the latter. Notice that we cannot assume the static limit for this exercise, and we find it simpler to work in momentum space. We start by analyzing the kinetic term in Eq. (4.2),

$$\hat{Z}'_{\mu\nu}\hat{Z}'^{\mu\nu} \xrightarrow{\text{mom. space}} -2\hat{Z}'_\mu(p^\mu p^\nu - p^2\eta^{\mu\nu})\hat{Z}'_\nu, \quad (4.7)$$

where p is the external momentum. We proceed in the same fashion when dealing with Eq. (4.3),

$$\hat{Z}'_{\mu\nu}\hat{B}^{\mu\nu} \xrightarrow{\text{mom. space}} -2\hat{Z}'_\mu(p^\mu p^\nu - p^2\eta^{\mu\nu})\hat{B}_\nu. \quad (4.8)$$

Thus the relevant pieces of the initial Lagrangian read

$$\mathcal{L} = \frac{1}{2}\hat{Z}'_\mu(p^\mu p^\nu - \eta^{\mu\nu}p^2 + \widehat{M}_{Z'}^2\eta^{\mu\nu})\hat{Z}'_\nu + \delta\widehat{M}^2\hat{Z}'_\mu\hat{Z}'^\mu + s_\chi\hat{Z}'_\mu(p^\mu p^\nu - p^2\eta^{\mu\nu})\hat{B}_\nu, \quad (4.9)$$

where $s_\chi \equiv \sin \chi$. The stationarity of the total action translates to

$$\frac{\delta \mathcal{L}}{\delta \hat{Z}'_\nu} = p^\mu p^\nu \hat{Z}'_\mu - p^2 \eta^{\mu\nu} \hat{Z}'_\mu + \widehat{M}_{Z'}^2 \eta^{\mu\nu} \hat{Z}'_\mu + \delta \widehat{M}^2 \eta^{\nu\rho} \hat{Z}_\rho + s_\chi (p^\nu p^\rho - p^2 \eta^{\nu\rho}) \hat{B}_\rho = 0, \quad (4.10)$$

$$\implies \left(p^\mu p^\nu - p^2 \eta^{\mu\nu} + \widehat{M}_{Z'}^2 \eta^{\mu\nu} \right) \hat{Z}'_\mu = -\delta \widehat{M}^2 \eta^{\nu\rho} \hat{Z}_\rho - s_\chi (p^\nu p^\rho - p^2 \eta^{\nu\rho}) \hat{B}_\rho. \quad (4.11)$$

To solve for the \hat{Z}' field, we use a procedure familiar from the derivation of the Proca propagator. This leads to

$$\begin{aligned} \hat{Z}'_\mu &= \frac{1}{p^2 - \widehat{M}_{Z'}^2} \left(\eta_{\mu\nu} - \frac{p_\mu p_\nu}{\widehat{M}_{Z'}^2} \right) \left(\delta \widehat{M}^2 \eta^{\nu\rho} \hat{Z}_\rho + s_\chi (p^\nu p^\rho - p^2 \eta^{\nu\rho}) \hat{B}_\rho \right) \\ &= \frac{1}{p^2 - \widehat{M}_{Z'}^2} \left(\delta \widehat{M}^2 \hat{Z}_\mu + s_\chi (p_\mu p^\rho \hat{B}_\rho - p^2 \hat{B}_\mu) - \frac{\delta \widehat{M}^2}{\widehat{M}_{Z'}^2} p_\mu p^\rho \hat{Z}_\rho \right). \end{aligned} \quad (4.12)$$

Now we plug this expression back into the initial Lagrangian, paying attention to write everything in the same basis, since in Eq. (4.3) we have both \hat{Z} and \hat{B} , where $\hat{Z} = \hat{c}_W \widehat{W}^3 - \hat{s}_W \hat{B}$. Here \hat{c}_W and \hat{s}_W denote respectively the cosine and sine of the weak mixing angle. The effective Lagrangian takes the form, after dropping terms that can be neglected due to Eq. (2.26),

$$\mathcal{L}_{\text{eff}} = -\frac{1}{2} \widehat{W}_\mu^3 \Pi_{33}(p^2) \widehat{W}^{3\mu} - \frac{1}{2} \hat{B}_\mu \Pi_{BB}(p^2) \hat{B}^\mu - \widehat{W}_\mu^3 \Pi_{3B}(p^2) \hat{B}^\mu + \dots, \quad (4.13)$$

with

$$\begin{cases} \Pi_{33}(p^2) = -\frac{1}{p^2 - \widehat{M}_{Z'}^2} \left(\delta \widehat{M}^2 \right)^2 \hat{c}_W^2, \\ \Pi_{3B}(p^2) = +\frac{1}{p^2 - \widehat{M}_{Z'}^2} \left[\hat{s}_W \hat{c}_W \left(\delta \widehat{M}^2 \right)^2 + \delta \widehat{M}^2 s_\chi p^2 \hat{c}_W \right], \\ \Pi_{BB}(p^2) = -\frac{1}{p^2 - \widehat{M}_{Z'}^2} \left[\left(\delta \widehat{M}^2 \right)^2 \hat{s}_W^2 + 2\delta \widehat{M}^2 s_\chi \hat{s}_W p^2 + s_\chi^2 p^4 \right]. \end{cases} \quad (4.14)$$

We now have all the ingredients to calculate the oblique parameters, for which we find by expanding in p^2

$$\hat{S} = \frac{g}{g'} \Pi'_{3B}(0) = -\frac{\hat{c}_W}{\hat{s}_W} \left[\hat{s}_W \hat{c}_W \frac{(\delta \widehat{M}^2)^2}{\widehat{M}_{Z'}^4} + s_\chi \hat{c}_W \frac{\delta \widehat{M}^2}{\widehat{M}_{Z'}^2} \right], \quad (4.15)$$

$$\hat{T} = \frac{\Pi_{33}(0) - \Pi_{W+W-}(0)}{M_W^2} = \frac{\hat{c}_W^2 (\delta \widehat{M}^2)^2}{M_W^2 \widehat{M}_{Z'}^2}, \quad (4.16)$$

$$\hat{U} = \Pi'_{W+W-}(0) - \Pi'_{33}(0) = -\hat{c}_W^2 \frac{(\delta \widehat{M}^2)^2}{\widehat{M}_{Z'}^4}, \quad (4.17)$$

$$V = \frac{M_W^2}{2} (\Pi''_{33}(0) - \Pi''_{W+W-}(0)) = \frac{\hat{c}_W^2 M_W^2 (\delta \widehat{M}^2)^2}{\widehat{M}_{Z'}^6}, \quad (4.18)$$

$$W = \frac{M_W^2}{2} \Pi''_{33}(0) = \frac{\hat{c}_W^2 M_W^2 (\delta \widehat{M}^2)^2}{\widehat{M}_{Z'}^6}, \quad (4.19)$$

$$X = \frac{M_W^2}{2} \Pi''_{3B}(0) = -M_W^2 \left(\frac{s_\chi \hat{c}_W \delta \widehat{M}^2}{\widehat{M}_{Z'}^4} + \frac{\hat{s}_W \hat{c}_W (\delta \widehat{M}^2)^2}{\widehat{M}_{Z'}^6} \right), \quad (4.20)$$

$$Y = \frac{M_W^2}{2} \Pi''_{BB}(0) = \frac{M_W^2}{\widehat{M}_{Z'}^2} \left(\frac{\widehat{s}_W \delta \widehat{M}^2}{\widehat{M}_{Z'}^2} + s_\chi \right)^2. \quad (4.21)$$

Notice that in this model we have simply $\Pi_{W+W-}(p^2) = 0$. We have boxed the 4 corrections that have been shown [41] to be sufficient to describe heavy universal new physics. The remaining 3 parameters have the same symmetries as some of the previous 4, but are subleading: for instance,

$$|\widehat{U}| \simeq \left(\frac{M_W^2}{\widehat{M}_{Z'}^2} \right) \widehat{T} \ll \widehat{T}. \quad (4.22)$$

Having calculated the oblique parameters, we now aim to set constraints on the Z' parameter space from EWPT data. To do so we construct a χ^2 fit, following closely Ref. [42]. While this is a relatively old study, the electroweak fit has not changed dramatically since then, so their results conveniently suffice to gain some initial insight on the problem. Calling p the theoretical parameters of the model, we build the χ^2 as follows,

$$\chi^2(p) = \sum_X \frac{(X_{\text{th}}(p) - X_{\text{exp}})^2}{\sigma_X^2}, \quad (4.23)$$

where the various quantities are defined [42] in the equation

$$R \cdot \underbrace{\begin{pmatrix} \widehat{S} \\ \widehat{T} \\ \widehat{U} \\ V \\ W \\ X \\ Y \\ \delta C_q \\ \delta \epsilon_b \\ \delta \epsilon_q \end{pmatrix}}_{X_{\text{th}}} = 10^{-3} \underbrace{\begin{pmatrix} 0.54l - 0.04 \\ 0.08l + 0.13 \\ 0.21l + 0.41 \\ 0.72l + 0.16 \\ -0.33l - 0.36 \\ 0.16l \\ -0.12l - 0.9 \\ -0.31l - 5.6 \\ 0.18l - 0.4 \\ 0.66l - 26 \end{pmatrix}}_{X_{\text{exp}}} \pm 10^{-3} \underbrace{\begin{pmatrix} 0.21 \\ 0.43 \\ 0.5 \\ 0.54 \\ 0.75 \\ 1.2 \\ 1.5 \\ 2.0 \\ 8.7 \\ 18 \end{pmatrix}}_{\sigma_X}, \quad (4.24)$$

where $l \equiv \log(m_h/M_Z) \approx 0.32$ (Ref. [42] was published well before the Higgs discovery, so m_h was left as a free parameter in their analysis), and

$$R = 10^{-3} \cdot \begin{pmatrix} -404 & 353 & -133 & 173 & 137 & -753 & 276 & 4 & 18 & 27 \\ -245 & -19 & 492 & -747 & 30 & -37 & 280 & 15 & -40 & -235 \\ -16 & 208 & 146 & -152 & -724 & -224 & -407 & 319 & 33 & 260 \\ -222 & 691 & -76 & 5 & -120 & 550 & 285 & -129 & 55 & 216 \\ -17 & -330 & 177 & -36 & 114 & -31 & 273 & -12 & 1 & 876 \\ 3 & 232 & -7 & -283 & 303 & -118 & -589 & -581 & -175 & 209 \\ -42 & -68 & 132 & 31 & -44 & -37 & -66 & -288 & 939 & -33 \\ -203 & -200 & 350 & 375 & -445 & -9 & 126 & -587 & -282 & -124 \\ -642 & -381 & -575 & -219 & -161 & 147 & -112 & -41 & 9 & 11 \\ 519 & 0 & -458 & -341 & -329 & -199 & 376 & -337 & -1 & 2 \end{pmatrix}. \quad (4.25)$$

These results were obtained from a fit to LEP1 and LEP2 data [42]. We include in the theoretical prediction our results for the 7 oblique parameters. This formalism also accounts for the (non-universal) vertex corrections δC_q , $\delta \epsilon_b$ and $\delta \epsilon_q$, which however vanish in our setup. We then use Eqs. (4.23) and (4.24) to build $\chi^2(\delta \widehat{M}^2, \widehat{M}_{Z'}, \sin \chi)$. The allowed regions of our input parameter are those satisfying

$$\chi^2 - \chi_{\min}^2 \leq \chi_{\text{critical}}^2, \quad (4.26)$$

where χ_{\min}^2 is the minimum of the χ^2 distribution and χ_{critical}^2 is a critical value that depends on the chosen confidence level and on the number of degrees of freedom. In our case we are going to fix $\sin \chi$

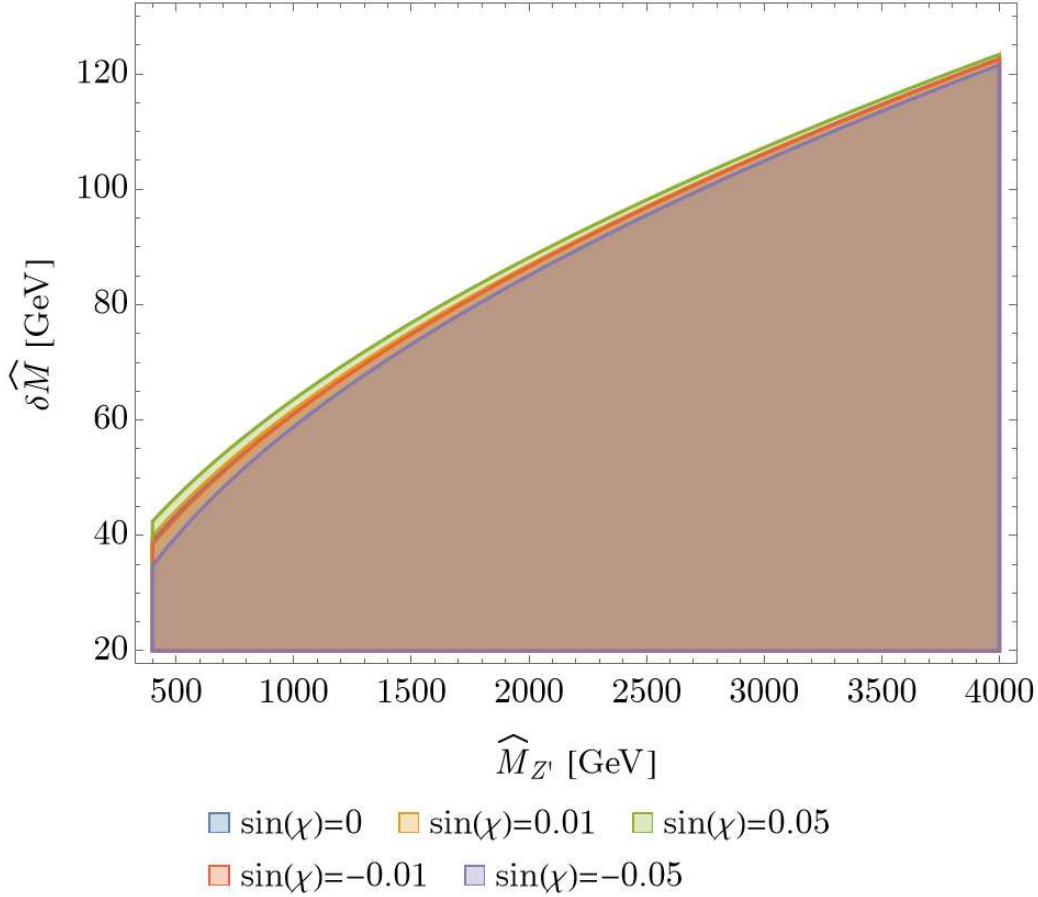


Figure 4.2: Allowed regions of the $\widehat{\delta M}$ versus $\widehat{M}_{Z'}$ parameter space at 95% CL. We have chosen to show results for different values of $\sin \chi$, corresponding to different colors.

to representative values, hence $\chi_{\text{critical}}^2 = 5.99$ for 95% CL and two degrees of freedom. The results are shown in Fig. 4.2, where $\widehat{\delta M}$ is plotted versus $\widehat{M}_{Z'}$, showing the allowed regions at 95% CL. We assume $\widehat{\delta M}^2 > 0$ for concreteness. This is a first original result of our work, showing quantitatively how large $\widehat{\delta M}^2$ can be as a function of the heavy Z' mass, while remaining consistent with EWPT. We notice that varying $\sin \chi$ has a moderate impact on the constraint. We conclude this part by mentioning that the opposite situation where the Z' is light – lighter than the SM Z – is also very interesting, and not experimentally ruled out. However, it requires an ad-hoc treatment of EWPT that goes beyond the scope of this thesis. We leave such study as a promising direction for future research.

4.2 Constraints from Z invisible decays

Other constraints on the model come from invisible decays of the Z boson, if we make the reasonable assumption that most of the produced dark hadrons leave the experimental apparatus undetected. In order to calculate the width for Z decay to dark fermions, we perform the diagonalization of the vector fields to the mass eigenstate basis. This will lead us to identify the physical spin-1 fields Z_1 and Z_2 , the former of which corresponds to the observed Z boson.

First we focus on the kinetic terms and perform the following field redefinition,

$$\begin{pmatrix} \widehat{B}_\mu \\ \widehat{Z}'_\mu \end{pmatrix} = \begin{pmatrix} 1 & -\tan \chi \\ 0 & 1/\cos \chi \end{pmatrix} \begin{pmatrix} B_\mu \\ Z'_\mu \end{pmatrix}. \quad (4.27)$$

Next, we remove the mixing of the massive bosons through a rotation,

$$\begin{pmatrix} A_\mu \\ Z_{\mu 1} \\ Z_{\mu 2} \end{pmatrix} = \begin{pmatrix} 1 & 0 & 0 \\ 0 & \cos \xi & \sin \xi \\ 0 & -\sin \xi & \cos \xi \end{pmatrix} \begin{pmatrix} A_\mu \\ Z_\mu \\ Z'_\mu \end{pmatrix} = \begin{pmatrix} \hat{c}_W & \hat{s}_W & 0 \\ -\hat{s}_W \cos \xi & \hat{c}_W \cos \xi & \sin \xi \\ \hat{s}_W \sin \xi & -\hat{c}_W \sin \xi & \cos \xi \end{pmatrix} \begin{pmatrix} B_\mu \\ W_\mu^3 \\ Z'_\mu \end{pmatrix}. \quad (4.28)$$

Putting all together we are able to relate the hatted basis $(\hat{A}_\mu, \hat{Z}_\mu, \hat{Z}'_\mu)$ with the $(A_\mu, Z_{\mu 1}, Z_{\mu 2})$ basis,

$$\begin{pmatrix} A_\mu \\ Z_{\mu 1} \\ Z_{\mu 2} \end{pmatrix} = \begin{pmatrix} 1 & 0 & \hat{c}_W \sin \chi \\ 0 & \cos \xi & -\hat{s}_W \cos \xi \sin \chi + \sin \xi \cos \chi \\ 0 & -\sin \xi & +\hat{s}_W \sin \xi \sin \chi + \cos \xi \cos \chi \end{pmatrix} \begin{pmatrix} \hat{A}_\mu \\ \hat{Z}_\mu \\ \hat{Z}'_\mu \end{pmatrix} \quad (4.29)$$

which can be inverted to obtain

$$\begin{pmatrix} \hat{A}_\mu \\ \hat{Z}_\mu \\ \hat{Z}'_\mu \end{pmatrix} = \underbrace{\begin{pmatrix} 1 & -\hat{c}_W \sin \xi \tan \chi & -\hat{c}_W \cos \xi \tan \chi \\ 0 & \cos \xi + \hat{s}_W \sin \xi \tan \chi & -\sin \xi + \hat{s}_W \cos \xi \tan \chi \\ 0 & \sin \xi / \cos \chi & \cos \xi / \cos \chi \end{pmatrix}}_L \begin{pmatrix} A_\mu \\ Z_{\mu 1} \\ Z_{\mu 2} \end{pmatrix}. \quad (4.30)$$

The mixing angle has the expression

$$\tan 2\xi = \frac{-2 \cos \chi (\delta \hat{M}^2 + \hat{s}_W \sin \chi \hat{M}_Z^2)}{\hat{M}_{Z'}^2 - \cos^2 \chi \hat{M}_Z^2 + \hat{s}_W^2 \sin^2 \chi \hat{M}_Z^2 + 2 \hat{s}_W \sin \chi \delta \hat{M}^2}. \quad (4.31)$$

Having removed all the mixing terms in Eq. (4.3), we now look at the interaction Lagrangian between the fermions and the physical vectors Z_1 and Z_2 . Recall that our original Lagrangian was

$$\begin{aligned} \mathcal{L} = & \frac{1}{2} \hat{M}_Z^2 \hat{Z}_\mu \hat{Z}^\mu + \frac{1}{2} \hat{M}_{Z'}^2 \hat{Z}'_\mu \hat{Z}'^\mu + \delta \hat{M}^2 \hat{Z}'_\mu \hat{Z}^\mu - \sum_f \frac{g}{\hat{c}_W} \hat{Z}_\mu \bar{f} \gamma^\mu \left(\frac{T_{Lf}^3 - 2 \hat{s}_W^2 Q_f}{2} - \frac{T_{Lf}^3}{2} \gamma_5 \right) f \\ & - e \sum_f \bar{f} Q_f \gamma^\mu f \hat{A}_\mu - g_D \sum_i (\bar{\psi}_{Li} X_{Li} \gamma^\mu \psi_{Li} + \bar{\psi}_{Ri} X_{Ri} \gamma^\mu \psi_{Ri}) \hat{Z}'_\mu, \end{aligned} \quad (4.32)$$

where kinetic terms are understood. Going to the mass eigenstate basis,

$$\mathcal{L} = \frac{1}{2} \begin{pmatrix} A & Z_1 & Z_2 \end{pmatrix} \begin{pmatrix} 0 & & \\ & M_{Z_1}^2 & \\ & & M_{Z_2}^2 \end{pmatrix} \begin{pmatrix} A \\ Z_1 \\ Z_2 \end{pmatrix} - \begin{pmatrix} e J_{\text{em}} & g_Z \hat{J}_Z & g_D J_D \end{pmatrix} L \begin{pmatrix} A \\ Z_1 \\ Z_2 \end{pmatrix}, \quad (4.33)$$

where $M_{Z_1} = M_Z$. Notice that the interactions of the photon are not modified with respect to the SM,

$$\mathcal{L}_{\text{QED}} = -e \bar{f} Q_f \gamma^\mu f A_\mu. \quad (4.34)$$

The interaction between the dark currents and the physical Z is now

$$\mathcal{L} \supset - \frac{\sin \xi}{\cos \chi} g_D J_D^\mu Z_{1\mu}. \quad (4.35)$$

As a last step, we need to go to the mass eigenstate basis for the dark fermions, as well. Performing unitary transforms that take us to the physical states, labeled ψ' , we obtain

$$\begin{aligned} J_D^\mu = & \bar{\psi}_L \mathbf{X}_L \gamma^\mu \psi_L + \bar{\psi}_R \mathbf{X}_R \gamma^\mu \psi_R \mapsto \bar{\psi}'_L \underbrace{U_L^\dagger \mathbf{X}_L U_L}_{\mathbf{X}'_L} \gamma^\mu \psi'_L + \bar{\psi}'_R \underbrace{U_R^\dagger \mathbf{X}_R U_R}_{\mathbf{X}'_R} \gamma^\mu \psi'_R \\ = & \bar{\psi}' \underbrace{\frac{\mathbf{X}'_L + \mathbf{X}'_R}{2}}_{\mathbf{X}'_V} \gamma^\mu \psi' + \bar{\psi}' \underbrace{\frac{\mathbf{X}'_R - \mathbf{X}'_L}{2}}_{\mathbf{X}'_A} \gamma^\mu \gamma_5 \psi', \end{aligned} \quad (4.36)$$

where we have adopted a matrix notation in dark flavor space. The Feynman amplitude for $Z_1 \rightarrow \bar{\psi}'_i \psi'_j$, where i, j denote flavor indices, reads

$$i\mathcal{M} = -i \frac{\sin \xi}{\cos \chi} g_D \bar{u}(q_1) (\mathbf{X}'_V \gamma^\mu + \mathbf{X}'_A \gamma^\mu \gamma_5)_{ij} v(q_2) \epsilon_\mu(p) \quad (4.37)$$

and by neglecting the masses of the dark quarks and summing over all flavors we arrive at

$$\begin{aligned} \Gamma(Z_1 \rightarrow \bar{\psi}' \psi') &= \frac{N_d g_D^2}{12\pi} \frac{\sin^2 \xi}{\cos^2 \chi} M_{Z_1} \text{Tr} [\mathbf{X}'_V (\mathbf{X}'_V)^\dagger + \mathbf{X}'_A (\mathbf{X}'_A)^\dagger] \\ &= \frac{N_d g_D^2}{24\pi} \frac{\sin^2 \xi}{\cos^2 \chi} M_{Z_1} \text{Tr} [\mathbf{X}_L (\mathbf{X}_L)^\dagger + \mathbf{X}_R (\mathbf{X}_R)^\dagger] \\ &= \frac{N_d g_D^2}{24\pi} \frac{\sin^2 \xi}{\cos^2 \chi} M_{Z_1} \sum_i (X_{Li}^2 + X_{Ri}^2), \end{aligned} \quad (4.38)$$

where N_d is the number of dark colors. In the last step, we have used the fact that in the initial basis the $U(1)'$ charge matrices can be taken as diagonal and real. Incidentally, we see how the decay width does not depend on the rotation matrices $U_{L,R}$: this result was to be expected, since we are summing over all dark quarks. From the above result we extract a constraint on the mixing angle ξ . Making the safe approximation that the kinetic mixing parameter is small, $\cos \chi \approx 1$, and recalling that the BSM invisible decay width of the Z must be less than 2 MeV [54], we find

$$\xi < 2.3 \times 10^{-2} \sqrt{\frac{3}{N_d}} \frac{1}{g_D \sqrt{\sum_i (X_{Li}^2 + X_{Ri}^2)}}. \quad (4.39)$$

This is another quantification of the allowed size of the mixing between Z and Z' , which can be compared to the results of our EWPT analysis. As reference values, we have fixed $N_d = 3$ (inspired by Neutral Naturalness ideas), and order one values for the $U(1)'$ charges and gauge coupling. Our discussion of constraints on the Z' model has come to a conclusion. In the next chapter, we take a closer look at the dark pion phenomenology expected in this setup.

Chapter 5

Dark pions in the Z' model

In this chapter we investigate the phenomenology of the dark pions in the Z' model introduced in the previous chapter. We assume $N = 2$ light flavors of dark quarks, the minimal choice for pNGBs to be present in the theory. At the qualitative level the dark pion properties are similar to the heavy fermion model reviewed in section 3.2, but the details of the mediation are different: the CP -odd pions can be viewed as ALPs coupled to the SM by the $Z - Z'$ portal, while the CP -even pions are light scalars connected to the SM via the $h - \phi$ portal. In section 5.1 we derive the expression of the effective decay constant for the CP -odd dark pions, $f_a^{(b)}$, which is one of the significant results of this thesis. In section 5.2 we discuss the properties of the CP -even pions.

5.1 The $Z - Z'$ portal for CP -odd dark pions

The first question we ask, is what expression the effective decay constant $f_a^{(b)}$ takes in the Z' model, and how it compares to the result found in the heavy fermion model, Eq. (3.12). To derive the answer we integrate out both Z_1 and Z_2 at tree level, obtaining an effective Lagrangian valid at the relevant energy scale $E \sim m_{\hat{\pi}} \ll M_{Z_{1,2}}$.

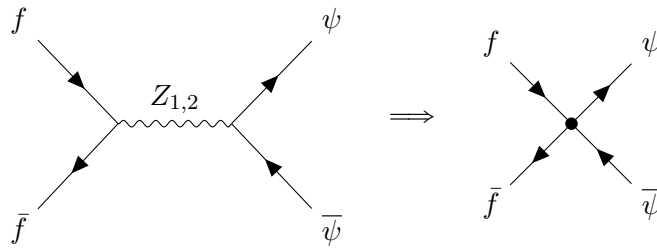


Figure 5.1: Diagrams illustrating the process of integrating out $Z_{1,2}$, producing effective 4-fermion interactions.

Solving the EOM and plugging back into the initial Lagrangian, we obtain

$$\mathcal{L}_{\text{eff}} = -\frac{1}{2} \begin{pmatrix} eJ_{\text{em}} & g_Z \hat{J}_Z & g_D J_D \end{pmatrix} L \begin{pmatrix} 0 & & \\ & M_{Z_1}^{-2} & \\ & & M_{Z_2}^{-2} \end{pmatrix} L^T \begin{pmatrix} eJ_{\text{em}} \\ g_Z \hat{J}_Z \\ g_D J_D \end{pmatrix}. \quad (5.1)$$

Since we are interested in four-fermion operators of the $\bar{f}f\bar{\psi}\psi$ type, we only keep the $J_D \times J_{\text{SM}}$ pieces,

$$\mathcal{L}_{\text{eff}} \supset -g_D J_D \left\{ \frac{L_{32}}{M_{Z_1}^2} \left(L_{12} eJ_{\text{em}} + L_{22} g_Z \hat{J}_Z \right) + \frac{L_{33}}{M_{Z_2}^2} \left(L_{13} eJ_{\text{em}} + L_{23} g_Z \hat{J}_Z \right) \right\} \quad (5.2)$$

Furthermore, recalling the discussion around Eq. (3.11), it is sufficient to retain the following terms,

$$\mathcal{L}_{\text{eff}} \supset \frac{1}{2} g_D g_Z T_{L_f}^3 \bar{f} \gamma^\mu \gamma_5 f \left(\frac{L_{32} L_{22}}{M_{Z_1}^2} + \frac{L_{33} L_{23}}{M_{Z_2}^2} \right) J_D. \quad (5.3)$$

We still need to simplify the sum in parentheses. By making use of the definitions of the L_{ij} in Eq. (4.30), we find

$$\begin{aligned} \frac{L_{32} L_{22}}{M_{Z_1}^2} + \frac{L_{33} L_{23}}{M_{Z_2}^2} &= \frac{-\sin \xi \cos \xi (M_{Z_1}^2 - M_{Z_2}^2) + \hat{s}_W \tan \chi (M_{Z_1}^2 \cos^2 \xi + M_{Z_2}^2 \sin^2 \xi)}{\cos \chi M_{Z_1}^2 M_{Z_2}^2} \\ &= -\frac{\delta \widehat{M}^2}{\cos^2 \chi M_{Z_1}^2 M_{Z_2}^2}, \end{aligned} \quad (5.4)$$

where in the last step we have made use of the exact relations

$$M_{Z_1}^2 \cos^2 \xi + M_{Z_2}^2 \sin^2 \xi = \widehat{M}_Z^2, \quad (M_{Z_1}^2 - M_{Z_2}^2) \sin \xi \cos \xi = \frac{\delta \widehat{M}^2}{\cos \chi} + \widehat{M}_Z^2 \hat{s}_W \tan \chi. \quad (5.5)$$

In summary, so far we have obtained

$$\mathcal{L}_{\text{eff}} \supset -\frac{1}{2} g_D g_Z T_{L_f}^3 \bar{f} \gamma^\mu \gamma_5 f \frac{\delta \widehat{M}^2}{\cos^2 \chi M_{Z_1}^2 M_{Z_2}^2} J_D. \quad (5.6)$$

The last step consists in replacing the axial part of J_D with $\text{Tr}(\sigma_b \mathbf{X}'_A) f_{\hat{\pi}} \partial^\mu \hat{\pi}_b$, following the same algebraic manipulations we performed around Eq. (3.7). The end result is

$$\mathcal{L}_{\text{eff}} \supset -\frac{1}{2} g_D g_Z \text{Tr}(\sigma_b \mathbf{X}'_A) f_{\hat{\pi}} \partial_\mu \hat{\pi}_b T_{L_f}^3 \bar{f} \gamma^\mu \gamma_5 f \frac{\delta \widehat{M}^2}{\cos^2 \chi M_{Z_1}^2 M_{Z_2}^2}, \quad (5.7)$$

which matches Eq. (3.12) with $c_f = T_{L_f}^3$ and

$$\frac{1}{f_a^{(b)}} = \frac{1}{2} g_D g_Z \text{Tr}(\sigma_b \mathbf{X}'_A) f_{\hat{\pi}} \frac{\delta \widehat{M}^2}{\cos^2 \chi M_{Z_1}^2 M_{Z_2}^2}. \quad (5.8)$$

This is one of our main results. We observe that the interaction vanishes when $\delta \widehat{M}^2 \rightarrow 0$. In other words, we find that kinetic mixing does not mediate the decay of the dark pions. With a little thought, we realize this was expected [57]: kinetic mixing only affects the transverse modes of gauge fields, and exchange of a single transverse vector cannot mediate the decay of a pion (another way to say this, is that $p_\mu (p^\mu p^\nu - p^2 \eta^{\mu\nu}) = 0$).

5.1.1 Comparing the two UV completions

Let us briefly compare the result we have just found for the Z' completion to the one for the completion including heavy fermions, Eq. (3.12). Assuming the traces over dimensionless matrices are $\mathcal{O}(1)$, we find the parametric estimates

$$\left(\frac{1}{f_a} \right)_{\text{fermions}} \sim \frac{Y^2 f_{\hat{\pi}}}{M^2} \quad (5.9)$$

for the heavy fermion model, where M denotes the mass scale of the Q states and we have set $\tilde{Y} = 0$ for simplicity, whereas in the Z' model

$$\left(\frac{1}{f_a} \right)_{Z'} \sim \frac{g_D g_Z f_{\hat{\pi}} \delta \widehat{M}^2}{M_{Z_2}^2 M_Z^2}. \quad (5.10)$$

If we now assume $g_D g_Z \sim Y^2$, which is quite reasonable since we expect all of these to be $\mathcal{O}(1)$ couplings, we find that for the same scale of new physics $M_{Z_2} \sim M$ the ratio of effective decay constants is

$$\frac{(f_a)_{\text{fermions}}}{(f_a)_{Z'}} \sim \frac{\delta \widehat{M}^2}{M_Z^2}. \quad (5.11)$$

Recalling the bounds from EWPT presented in Fig. 4.2, we conclude that f_a needs to be slightly larger in the Z' completion, by a modest amount. For instance, for $M_{Z_2} = 1$ TeV the 95% CL constraint from EWPT is $\delta \widehat{M}^2 / \widehat{M}_Z^2 < 0.30$. The situation changes if the Z' is light but, as already mentioned, we leave a discussion of that regime to future work.

5.1.2 A concrete example model

To gain some additional insight, we write down a concrete model with $N = 2$ dark flavors. The $U(1)'$ charges are chosen as follows,

$$\begin{cases} X_{1L} = X_{1R} \equiv X_1 \\ X_{2L} = X_{2R} \equiv X_2 \end{cases}. \quad (5.12)$$

This automatically makes the theory anomaly-free. We also assume that the scalar Φ has charge $X_\Phi = X_1 - X_2$, so that the following dark Yukawa Lagrangian is invariant under $U(1)'$,

$$\mathcal{L} = -y_1 \bar{\psi}_{1L} \psi_{2R} \Phi - y_2 \bar{\psi}_{2L} \psi_{1R} \Phi^* + \text{h.c.} \quad (5.13)$$

Furthermore, taking $\mathbf{m} = \text{diag}(m_1, m_2)$, the total mass Lagrangian can be written in matrix form as

$$\mathcal{L}_{\text{mass}}^{\text{tot}} = -(\bar{\psi}_{1L} \quad \bar{\psi}_{2L}) \underbrace{\begin{pmatrix} m_1 & y_1 \Phi \\ y_2 \Phi^* & m_2 \end{pmatrix}}_{\mathbf{h}} \begin{pmatrix} \psi_{1R} \\ \psi_{2R} \end{pmatrix} + \text{h.c.} \quad (5.14)$$

In general, all the entries of the matrix \mathbf{h} are complex quantities. We then ask ourselves how many of the 4 complex phases that appear in this matrix can be reabsorbed by field redefinitions. It is easy to see that after 3 entries are made real by rephasing the fermion fields, the freedom at our disposal is exhausted. This leaves us, in general, with one physical CP -violating phase. We should also note that, unless one quark is massless [5], the dark sector suffers from a strong CP problem analogous to the one of the SM. Here we do not tackle this aspect, simply disregarding the CP -violating phase of dark QCD.

For simplicity, we make a further simplification and assume $y_2 = 0$, which guarantees CP conservation of the Lagrangian. In this case the (real) mass Lagrangian reads

$$\langle \mathbf{h} \rangle = \begin{pmatrix} m_1 & y_1 v_\Phi \\ 0 & m_2 \end{pmatrix}, \quad (5.15)$$

which can be diagonalized to \mathbf{M} via orthogonal transformations,

$$\mathbf{M} = R^\dagger(\theta_L) \langle \mathbf{h} \rangle R(\theta_R), \quad (5.16)$$

where

$$R(\theta) \equiv \begin{pmatrix} \cos \theta & -\sin \theta \\ \sin \theta & \cos \theta \end{pmatrix}. \quad (5.17)$$

In order to evaluate the dark pion decay constant in Eq. (5.8) we need the expression of the matrix \mathbf{X}'_A ,

$$\begin{aligned} \mathbf{X}'_A &= \frac{1}{2} \left[R(-\theta_R) \begin{pmatrix} X_1 & \\ & X_2 \end{pmatrix} R(\theta_R) - R(-\theta_L) \begin{pmatrix} X_1 & \\ & X_2 \end{pmatrix} R(\theta_L) \right] \\ &= \frac{X_1 - X_2}{4} \begin{pmatrix} \cos 2\theta_R - \cos 2\theta_L & \sin 2\theta_L - \sin 2\theta_R \\ \sin 2\theta_L - \sin 2\theta_R & \cos 2\theta_L - \cos 2\theta_R \end{pmatrix}, \end{aligned} \quad (5.18)$$

from which the traces are evaluated,

$$\text{Tr}[\sigma_1 \mathbf{X}'_A] = \frac{1}{2} (X_1 - X_2) (\sin 2\theta_L - \sin 2\theta_R) , \quad (5.19)$$

$$\text{Tr}[\sigma_2 \mathbf{X}'_A] = 0 , \quad (5.20)$$

$$\text{Tr}[\sigma_3 \mathbf{X}'_A] = \frac{1}{2} (X_1 - X_2) (\cos 2\theta_R - \cos 2\theta_L) . \quad (5.21)$$

We find a zero trace for $\hat{\pi}_2$ because the model preserves CP , and CP -even dark pions cannot decay through the $Z - Z'$ portal.

To better illustrate our findings, we consider two specific sub-cases of Eq. (5.15) that produce simple analytical results:

- ($m_2 = 0$) In this case one quark is massless¹. Paying attention to some subtleties in the diagonalization of the mass matrix, which require in some parameter regimes to alter the definition of the rotation matrices with respect to the one given above, we find

$$\text{Tr}[\sigma_1 \mathbf{X}'_A] = \text{sgn}(y_1 v_\Phi - m_1) (X_1 - X_2) \frac{m_1 y_1 v_\Phi}{m_1^2 + y_1^2 v_\Phi^2} , \quad (5.22)$$

$$\text{Tr}[\sigma_3 \mathbf{X}'_A] = - (X_1 - X_2) \frac{y_1^2 v_\Phi^2}{m_1^2 + y_1^2 v_\Phi^2} . \quad (5.23)$$

We see that the effective decay constants of $\hat{\pi}_1$ and $\hat{\pi}_3$ are similar if $m_1 \sim y_1 v_\Phi$ is realized.

- ($m_2 = m_1$) Again we must pay attention to perform the correct diagonalization of the mass matrices. The result is

$$\text{Tr}[\sigma_1 \mathbf{X}'_A] = 0 , \quad (5.24)$$

$$\text{Tr}[\sigma_3 \mathbf{X}'_A] = - \frac{(X_1 - X_2)}{\sqrt{\frac{4m_1^2}{y_1^2 v_\Phi^2} + 1}} . \quad (5.25)$$

In this scenario, the decay of $\hat{\pi}_1$ via the $Z - Z'$ portal is accidentally forbidden.

5.2 The $h - \phi$ portal for CP -even dark pions

In the Z' model, the CP -even dark pions (namely $\hat{\pi}_2$, in the $N = 2$ scenario with CP conservation) decay to the SM by mixing with the Higgs boson and the radial mode ϕ of the $U(1)'$ -charged complex scalar Φ , which in unitary gauge reads $\Phi = v_\Phi + \phi/\sqrt{2}$. It is important to stress that in this thesis we assume the physical degrees of freedom belonging to the second Higgs doublet H' (which carries nonzero $U(1)'$ charge, in order to generate $\delta\hat{M}^2$) to be heavy and decoupled. Our starting point is Eq. (4.4), which we repeat here for convenience,

$$\mathcal{L}_\Phi = -\zeta_{ij} \bar{\psi}_{Li} \psi_{Rj} \Phi + \text{h.c.} - \kappa \Phi^* \Phi H^\dagger H . \quad (5.26)$$

The term proportional to κ is responsible for a mass mixing between the Higgs boson h and ϕ , which is diagonalized by a rotation with angle

$$\tan 2\theta_s \simeq \frac{2\sqrt{2}\kappa v_\Phi v}{m_h^2 - m_\phi^2} . \quad (5.27)$$

The rotation of h and ϕ results in an interaction between the physical Higgs field and the dark quarks,

$$\mathcal{L} \supset -\frac{\zeta_{ij}}{\sqrt{2}} \sin \theta_s \bar{\psi}_{Li} \psi_{Rj} h_{\text{phys}} + \text{h.c.} , \quad (5.28)$$

¹Note that in this case the strong CP problem of dark QCD would be automatically solved.

which mediates Higgs decay to dark fermions, with

$$\Gamma(h_{\text{phys}} \rightarrow \bar{\psi}\psi) \simeq \frac{N_d m_h}{16\pi} \text{Tr}(\zeta\zeta^\dagger) \sin^2 \theta_s. \quad (5.29)$$

The branching ratio of the Higgs invisible decays must be smaller than 0.13 at 95% CL [55], yielding the bound²

$$N_d \text{Tr}(\zeta\zeta^\dagger) \sin^2 \theta_s < 2 \times 10^{-4}. \quad (5.31)$$

At energies $E \ll m_h, m_\phi$, it is possible to integrate out the h and ϕ , leading to an effective Lagrangian coupling dark fermions and SM fermions,

$$\mathcal{L}_{\text{eff}} \supset -\frac{y_f}{2} \sin \theta_s \cos \theta_s \left(\frac{1}{m_\phi^2} - \frac{1}{m_h^2} \right) (\zeta_{ij} \bar{\psi}_{Li} \psi_{Rj} + \text{h.c.}) \bar{f} f. \quad (5.32)$$

After moving to the mass eigenbasis for the dark fermions, we obtain

$$\mathcal{L}_{\text{eff}} \supset -\frac{y_f}{2\sqrt{2}} \frac{\sin \theta_s \cos \theta_s (m_h^2 - m_\phi^2)}{\sqrt{2} m_h^2 m_\phi^2} \left[\bar{\psi}' (\mathbf{C}_s + \mathbf{C}_s^\dagger + (\mathbf{C}_s - \mathbf{C}_s^\dagger) \gamma_5) \psi' \right] \bar{f} f, \quad (5.33)$$

with

$$\mathbf{C}_s = U_L^\dagger \zeta U_R. \quad (5.34)$$

Finally, we translate the result to the hadronic basis. Since a 2×2 anti-hermitian matrix can be decomposed as

$$\mathbf{C}_s - \mathbf{C}_s^\dagger = -\sum_{q=0}^3 \text{Tr} [i\sigma_q (\mathbf{C}_s - \mathbf{C}_s^\dagger)] \frac{i\sigma_q}{2}, \quad (5.35)$$

we obtain a coupling

$$-\frac{\hat{B}_0 f_{\hat{\pi}} \kappa v_\Phi v}{2 m_h^2 m_\phi^2} \frac{y_f}{\sqrt{2}} \text{Tr} [i\sigma_b (\mathbf{C}_s - \mathbf{C}_s^\dagger)] \hat{\pi}_b \bar{f} f. \quad (5.36)$$

To conclude, we specialize the above results to the concrete example model presented in section 5.1.2. In the unitary gauge, where the angular mode of Φ has been eaten by the Z' , we can identify

$$\zeta = \begin{pmatrix} 0 & y_1 \\ y_2 & 0 \end{pmatrix}. \quad (5.37)$$

In our assumed limit $y_2 = 0$, CP is conserved. Therefore, the only non-vanishing trace is the one associated with $\hat{\pi}_2$. In the two simple cases we discussed before, we find

- ($m_2 = 0$)

$$\text{Tr} [i\sigma_2 (\mathbf{C}_s - \mathbf{C}_s^\dagger)] = \text{sgn}(y_1 v_\Phi - m_1) \frac{2y_1 m_1}{\sqrt{y_1^2 v_\Phi^2 + m_1^2}}; \quad (5.38)$$

- ($m_2 = m_1$)

$$\text{Tr} [i\sigma_2 (\mathbf{C}_s - \mathbf{C}_s^\dagger)] = -\frac{4y_1 m_1}{\sqrt{y_1^2 v_\Phi^2 + 4m_1^2}}. \quad (5.39)$$

These results conclude our first look at the Z' model. While a lot more remains to be done, they will provide the basis for future investigations of this scenario and of the associated phenomenology, both in the regime where the Z' is heavy, as assumed here, and in the yet-unexplored regime where the Z' is light.

²If $m_\phi < m_h/2$ (which is not likely to be verified in the parameter regions considered in this thesis, but may happen if the Z' is light), the κ term in Eq. (5.26) also mediates the $h \rightarrow \phi\phi$ decay, whose width is

$$\Gamma(h \rightarrow \phi\phi) = \frac{\kappa^2 v^2}{32\pi m_h} \left(1 - 4 \frac{m_\phi^2}{m_h^2} \right)^{1/2}. \quad (5.30)$$

Chapter 6

Conclusions

The discovery of the Higgs boson in 2012 marked the start of a new era for particle physics. It completed the SM, but at the same time it exacerbated the naturalness problem of its scalar sector. If the SM is coupled to new dynamics at some high energy scale – which appears unavoidable, given the many open questions the SM does not have an answer for – then the Higgs mass is highly sensitive to large quantum corrections and can be made as small as experimentally observed only at the price of fine tuning.

Robust solutions to this naturalness (or hierarchy) problem, based on symmetry principles, have been known for decades. While very different from each other, both classes of these “traditional” solutions (namely SUSY and compositeness, the latter invoking a description of the Higgs as pNGB) shared a central phenomenological prediction: new particles carrying QCD color should be found below the TeV. The LHC Runs 1 and 2 (as well as the initial portion of Run 3) have searched extensively for such states but have come back empty-handed, pushing the bounds on QCD-charged new particles into the 1.2 TeV to 1.5 TeV range depending on the specific realization, as we reviewed in chapter 1.

The lesson we have learned from these developments, is that an adjustment in perspective is likely necessary. In this thesis we have adopted a conservative point of view: perhaps the big picture we have built concerning the hierarchy problem and its symmetry-based solutions is correct, but we have missed some important details of the concrete realization. The Neutral Naturalness (NN) framework materializes this approach, by building models where the new particles appearing at the TeV are not charged under QCD color (and sometimes, under any of the SM gauge symmetries). This ameliorates significantly the naturalness of the Higgs mass, allowing the top partners to be quite light without conflicting with any experimental constraints from the LHC.

As we discussed in chapter 1, the best-known example of NN model is the Twin Higgs, where the Higgs boson appears as one of the pNGBs arising from an $SU(4)/SU(3)$ spontaneous symmetry breaking at scale $f \sim \text{TeV}$. A discrete symmetry exchanging the SM and Twin sectors ensures the cancellation of the quadratic corrections to the Higgs mass. Logarithmic corrections do not cancel, but are kept to an acceptable level for a solution to the little hierarchy problem up to $\Lambda \lesssim 4\pi f$. Importantly, 2-loop naturalness arguments suggest that Twin QCD should be a gauge symmetry, and that it should confine at a scale not far from that of SM QCD, namely around the GeV scale. This is a powerful, and generic, prediction of NN: in this framework, we expect a dark QCD to exist around the GeV scale. A set of portal interactions, including at least the Higgs boson, can allow us to access the dark sector and potentially give rise to spectacular signals, if some of the dark hadrons decay back to the SM.

In chapter 2 we introduced some useful theoretical prerequisites, namely chiral perturbation theory and the electroweak precision tests (EWPT) of the SM. Then, in chapter 3 we presented the main ideas about confining dark sectors. At first, we introduced the concrete dark QCD setup that is realized in the Fraternal Twin Higgs model (namely a minimal implementation of the Twin Higgs, where the first two generations of the SM are not twinned) and the most salient features of its phenomenology.

However, we also observed that the space of NN-motivated or -inspired dark sectors is far wider, and moved on to present a different class, which is the main subject of this thesis. It consists of models where the dark sector contains $N \geq 2$ dark flavors, so that pNGB pseudoscalar mesons sit at the bottom of the dark hadron spectrum, and the interactions between the SM and dark sectors are mediated by the Z boson (in addition to the Higgs boson). This scenario found its inception in a complete NN model (based on accidental SUSY of the mass spectrum), but is considered here in a bottom-up approach, without specifically requiring a solution to the little hierarchy problem. It can be UV-completed in two ways: either by invoking heavy fermions carrying both SM electroweak and dark QCD color charges, or by introducing a Z' vector that mixes with the SM gauge bosons.

After reviewing the first class of UV completion in chapter 3, and highlighting the use of ChPT techniques in extracting phenomenological predictions for light new particles coupled to the SM quarks, in chapter 4 we introduced the second class of UV completions, which has not been studied previously in the literature and is the main novelty of this thesis. We wrote down the model Lagrangian and proceeded to calculate the constraints on the parameter space that stem from EWPT. We also evaluated the constraints arising from Z invisible decays, which apply in large regions of parameter space, as the dark pions tend to be rather long lived compared to the length scales of accelerator experiments. We found that, in the region of TeV-scale Z' we are interested in here, EWPT constraints require the mixing mass term $\delta\widehat{M}^2 \lesssim (100 \text{ GeV})^2$. Our analysis allows one to easily derive precise bounds, for any values of the model parameters.

In chapter 5 we discussed the properties of dark pions in the Z' model. In particular, we calculated the value of the effective decay constant $f_a^{(b)}$ for the CP -odd dark pions, which decay via the $Z - Z'$ portal. As expected on general grounds, we found that only mass mixing mediates this decay, whereas kinetic mixing does not contribute. We also discussed the key features of the CP -even dark pions, whose decay is mediated by the SM-like h and by the radial mode ϕ of the complex scalar that gives the Z' its mass.

The original results we presented in chapter 4 and chapter 5 only scratch the surface in the analysis of the Z' UV completion of the Z portal. Nevertheless, we hope they will provide a useful basis for future studies. We conclude by mentioning some aspects that we believe deserve future attention. The first is a study of the phenomenological signatures of the model, focusing especially on the interplay between Z decays to “dark jets” made of dark pions at LHC Run 3 and beyond, and searches for rare decays of B mesons at Belle II. The second is a discussion of the regime where the Z' is light – possibly lighter than the Z . This requires a dedicated analysis of EWPT that has, to our knowledge, not appeared yet in the literature. While it goes beyond the scope of this thesis, we view it as an interesting avenue for future research.

Bibliography

- [1] ATLAS. Observation of a new particle in the search for the Standard Model Higgs boson with the ATLAS detector at the LHC. *Physics Letters B* **716**, 1–29 (2012). URL <https://doi.org/10.1016/j.physletb.2012.08.020>.
- [2] CMS. Observation of a new boson at a mass of 125 GeV with the CMS experiment at the LHC. *Physics Letters B* **716**, 30–61 (2012). URL <https://doi.org/10.1016%2Fj.physletb.2012.08.021>.
- [3] Weinheimer, C. & Zuber, K. Neutrino Masses. *Annalen der Physik* **525**, 565–575 (2013). URL <https://doi.org/10.1002%2Fandp.201300063>.
- [4] Feruglio, F., Hagedorn, C., Lin, Y. & Merlo, L. Theory of the neutrino mass (2008). URL <https://arxiv.org/abs/0808.0812>. 0808.0812.
- [5] Hook, A. TASI Lectures on the Strong CP Problem and Axions (2021). URL <https://arxiv.org/abs/1812.02669>. 1812.02669.
- [6] Peccei, R. D. The strong CP problem and axions. In *Lecture Notes in Physics*, 3–17 (Springer Berlin Heidelberg, 2008). URL https://doi.org/10.1007%2F978-3-540-73518-2_1.
- [7] Cline, J. M. Baryogenesis (2006). URL <https://arxiv.org/abs/hep-ph/0609145>. hep-ph/0609145.
- [8] Davidson, S., Nardi, E. & Nir, Y. Leptogenesis. *Physics Reports* **466**, 105–177 (2008). URL <https://doi.org/10.1016%2Fj.physrep.2008.06.002>.
- [9] Craig, N. Naturalness and new approaches to the hierarchy problem (2017). URL <https://www.ias.edu/sites/default/files/pitp/craig.pdf>.
- [10] Gaillard, M. K. & Lee, B. W. Rare decay modes of the K mesons in gauge theories. *Phys. Rev. D* **10**, 897–916 (1974). URL <https://link.aps.org/doi/10.1103/PhysRevD.10.897>.
- [11] Giudice, G. Naturally speaking: The naturalness criterion and physics at the LHC (2008). URL <https://arxiv.org/pdf/0801.2562.pdf>. 0801.2562.
- [12] Martin, S. P. A supersymmetry primer URL <https://arxiv.org/pdf/hep-ph/9709356.pdf>. hep-ph/9709356.
- [13] Schmaltz, M. & Tucker-Smith, D. Little Higgs Review. *Ann.Rev.Nucl.Part.Sci.* **55**, 229–270 (2005). URL <https://arxiv.org/pdf/hep-ph/0502182.pdf>. hep-ph/0502182.
- [14] Panico, G. & Wulzer, A. The Composite Nambu-Goldstone Higgs (2015). URL <https://arxiv.org/pdf/1506.01961.pdf>. 1506.01961.
- [15] ATLAS SUSY March 2023 Summary Plot Update. Tech. Rep., CERN, Geneva (2023). URL <http://cds.cern.ch/record/2852738>.
- [16] CMS B2G group. Public Physics Results. URL <https://twiki.cern.ch/twiki/bin/view/CMSPublic/PhysicsResultsB2G>.

- [17] Chacko, Z., Goh, H.-S. & Harnik, R. Natural electroweak breaking from a mirror symmetry. *Physical Review Letters* **96** (2006). URL <https://doi.org/10.1103/PhysRevLett.96.231802>.
- [18] Burdman, G., Chacko, Z., Goh, H.-S. & Harnik, R. Folded Supersymmetry and the LEP Paradox. *SLAC-PUB-12115* URL <https://arxiv.org/pdf/hep-ph/0609152.pdf>. hep-ph/0609152.
- [19] Craig, N., Knapen, S. & Longhi, P. Neutral Naturalness from Orbifold Higgs Models. *Phys. Rev. Lett.* **114**, 061803 (2015). URL <https://arxiv.org/pdf/1410.6808.pdf>. 1410.6808.
- [20] Craig, N., Knapen, S. & Longhi, P. The Orbifold Higgs. *JHEP* **03**, 106 (2015). URL [https://doi.org/10.1007/JHEP03\(2015\)106](https://doi.org/10.1007/JHEP03(2015)106). 1411.7393.
- [21] Craig, N., Katz, A., Strassler, M. & Sundrum, R. Naturalness in the Dark at the LHC. *JHEP* **07**, 105 (2015). URL [https://doi.org/10.1007/JHEP07\(2015\)105](https://doi.org/10.1007/JHEP07(2015)105). 1501.05310.
- [22] Barbieri, R., Greco, D., Rattazzi, R. & Wulzer, A. The Composite Twin Higgs scenario. *JHEP* **08**, 161 (2015). URL <https://arxiv.org/pdf/1501.07803.pdf>. 1501.07803.
- [23] Low, M., Tesi, A. & Wang, L.-T. Twin Higgs mechanism and a composite Higgs boson. *Phys. Rev. D* **91**, 095012 (2015). URL <https://doi.org/10.1103/PhysRevD.91.095012>. 1501.07890.
- [24] Craig, N. & Katz, A. The Fraternal WIMP Miracle. *JCAP* **10**, 054 (2015). URL <https://iopscience.iop.org/article/10.1088/1475-7516/2015/10/054/pdf>. 1505.07113.
- [25] Cohen, T., Craig, N., Lou, H. K. & Pinner, D. Folded Supersymmetry with a Twist. *JHEP* **03**, 196 (2016). URL [https://link.springer.com/content/pdf/10.1007/JHEP03\(2016\)196.pdf](https://link.springer.com/content/pdf/10.1007/JHEP03(2016)196.pdf). 1508.05396.
- [26] Cheng, H.-C., Jung, S., Salvioni, E. & Tsai, Y. Exotic quarks in Twin Higgs models. *Journal of High Energy Physics* **2016** (2016). URL <https://doi.org/10.1007/2Fjhep03%282016%29074>.
- [27] Craig, N., Knapen, S., Longhi, P. & Strassler, M. The Vector-like Twin Higgs. *JHEP* **07**, 002 (2016). URL [https://doi.org/10.1007/JHEP07\(2016\)002](https://doi.org/10.1007/JHEP07(2016)002). 1601.07181.
- [28] Cheng, H.-C., Li, L., Salvioni, E. & Verhaaren, C. B. Singlet Scalar Top Partners from Accidental Supersymmetry. *JHEP* **05**, 057 (2018). URL [https://doi.org/10.1007/JHEP05\(2018\)057](https://doi.org/10.1007/JHEP05(2018)057). 1803.03651.
- [29] Cohen, T., Craig, N., Giudice, G. F. & McCullough, M. The Hyperbolic Higgs. *JHEP* **05**, 091 (2018). URL [https://doi.org/10.1007/JHEP05\(2018\)091](https://doi.org/10.1007/JHEP05(2018)091). 1803.03647.
- [30] Borsato, M. *et al.* Unleashing the full power of LHCb to probe stealth new physics. *Rept. Prog. Phys.* **85**, 024201 (2022). URL <https://doi.org/10.1088/1361-6633/ac4649>. 2105.12668.
- [31] Knapen, S., Shelton, J. & Xu, D. Perturbative benchmark models for a dark shower search program. *Phys. Rev. D* **103**, 115013 (2021). URL <https://doi.org/10.1103/PhysRevD.103.115013>. 2103.01238.
- [32] Cheng, H.-C., Li, L. & Salvioni, E. A theory of dark pions. *Journal of High Energy Physics* **2022** (2022). URL [https://doi.org/10.1007/jhep01\(2022\)122](https://doi.org/10.1007/jhep01(2022)122).
- [33] Bernreuther, E. *et al.* Forecasting dark showers at Belle II. *JHEP* **12**, 005 (2022). URL [https://doi.org/10.1007/JHEP12\(2022\)005](https://doi.org/10.1007/JHEP12(2022)005). 2203.08824.
- [34] Born, S., Karur, R., Knapen, S. & Shelton, J. Scouting for dark showers at CMS and LHCb (2023). URL <https://arxiv.org/pdf/2303.04167.pdf>. 2303.04167.
- [35] Durieux, G., McCullough, M. & Salvioni, E. Gegenbauer’s Twin. *JHEP* **05**, 140 (2022). URL [https://doi.org/10.1007/JHEP05\(2022\)140](https://doi.org/10.1007/JHEP05(2022)140). 2202.01228.
- [36] Workman, R. L. *et al.* Review of Particle Physics. *PTEP* **2022**, 083C01 (2022). URL <https://doi.org/10.1093/ptep/ptac097>.

-
- [37] Chacko, Z., Craig, N., Fox, P. J. & Harnik, R. Cosmology in Mirror Twin Higgs and Neutrino Masses. *JHEP* **07**, 023 (2017). URL [https://doi.org/10.1007/JHEP07\(2017\)023](https://doi.org/10.1007/JHEP07(2017)023). 1611.07975.
 - [38] Scherer, S. Introduction to chiral perturbation theory. *Adv. Nucl. Phys.* **27**, 277 (2003). URL <https://arxiv.org/pdf/hep-ph/0210398.pdf>. hep-ph/0210398.
 - [39] Kaplan, D. B. Five lectures on effective field theory (2005). URL <https://arxiv.org/abs/nucl-th/0510023>. nucl-th/0510023.
 - [40] Babu, K. S., Kolda, C. F. & March-Russell, J. Implications of generalized $Z - Z'$ mixing. *Phys. Rev. D* **57**, 6788–6792 (1998). URL <https://doi.org/10.1103/PhysRevD.57.6788>. hep-ph/9710441.
 - [41] Barbieri, R., Pomarol, A., Rattazzi, R. & Strumia, A. Electroweak symmetry breaking after LEP-1 and LEP-2. *Nucl. Phys. B* **703**, 127–146 (2004). URL <https://doi.org/10.1016/j.nuclphysb.2004.10.014>. hep-ph/0405040.
 - [42] Cacciapaglia, G., Csaki, C., Marandella, G. & Strumia, A. The Minimal Set of Electroweak Precision Parameters. *Phys. Rev. D* **74**, 033011 (2006). URL <https://doi.org/10.1103/PhysRevD.74.033011>. hep-ph/0604111.
 - [43] Peskin, M. E. & Takeuchi, T. A New constraint on a strongly interacting Higgs sector. *Phys. Rev. Lett.* **65**, 964–967 (1990). URL <https://doi.org/10.1103/PhysRevLett.65.964>.
 - [44] Peskin, M. E. & Takeuchi, T. Estimation of oblique electroweak corrections. *Phys. Rev. D* **46**, 381–409 (1992). URL <https://link.aps.org/doi/10.1103/PhysRevD.46.381>.
 - [45] Cheng, H.-C., Li, L., Salvioni, E. & Verhaaren, C. B. Light Hidden Mesons through the Z Portal. *JHEP* **11**, 031 (2019). URL [https://doi.org/10.1007/JHEP11\(2019\)031](https://doi.org/10.1007/JHEP11(2019)031). 1906.02198.
 - [46] Morningstar, C. J. & Peardon, M. J. The Glueball spectrum from an anisotropic lattice study. *Phys. Rev. D* **60**, 034509 (1999). URL <https://doi.org/10.1103/PhysRevD.60.034509>. hep-lat/9901004.
 - [47] Chen, Y. *et al.* Glueball spectrum and matrix elements on anisotropic lattices. *Phys. Rev. D* **73**, 014516 (2006). URL <https://doi.org/10.1103/PhysRevD.73.014516>. hep-lat/0510074.
 - [48] Farchioni, F. *et al.* Hadron masses in QCD with one quark flavour. *Eur. Phys. J. C* **52**, 305–314 (2007). URL <https://doi.org/10.1140/epjc/s10052-007-0394-4>. 0706.1131.
 - [49] Curtin, D. & Verhaaren, C. B. Discovering Uncolored Naturalness in Exotic Higgs Decays. *JHEP* **12**, 072 (2015). URL [https://doi.org/10.1007/JHEP12\(2015\)072](https://doi.org/10.1007/JHEP12(2015)072). 1506.06141.
 - [50] Batell, B., Low, M., Neil, E. T. & Verhaaren, C. B. Review of Neutral Naturalness. In *Snowmass 2021* (2022). URL <https://arxiv.org/pdf/2203.05531.pdf>. 2203.05531.
 - [51] Cheng, H.-C., Salvioni, E. & Tsai, Y. Exotic electroweak signals in the twin Higgs model. *Phys. Rev. D* **95**, 115035 (2017). URL <https://doi.org/10.1103/PhysRevD.95.115035>. 1612.03176.
 - [52] Alimena, J. *et al.* Searching for long-lived particles beyond the Standard Model at the Large Hadron Collider. *J. Phys. G* **47**, 090501 (2020). URL <https://doi.org/10.1088/1361-6471/ab4574>. 1903.04497.
 - [53] Winkler, M. W. Decay and detection of a light scalar boson mixing with the Higgs boson. *Phys. Rev. D* **99**, 015018 (2019). URL <https://doi.org/10.1103/PhysRevD.99.015018>. 1809.01876.
 - [54] Precision electroweak measurements on the Z resonance. *Physics Reports* **427**, 257–454 (2006). URL <https://doi.org/10.1016%2Fj.physrep.2005.12.006>.

- [55] Search for invisible Higgs boson decays with vector boson fusion signatures with the ATLAS detector using an integrated luminosity of 139 fb^{-1} (2020). URL <https://doi.org/10.1007/JHEP08%282022%29104>.
- [56] Aloni, D., Soreq, Y. & Williams, M. Coupling QCD-scale axionlike particles to gluons. *Physical Review Letters* **123** (2019). URL <https://doi.org/10.1103/PhysRevLett.123.031803>.
- [57] Essig, R., Schuster, P. & Toro, N. Probing Dark Forces and Light Hidden Sectors at Low-Energy e^+e^- Colliders. *Phys. Rev. D* **80**, 015003 (2009). URL <https://doi.org/10.1103/PhysRevD.80.015003>. 0903.3941.